FRESH, MECHANICAL, DURABILITY AND CORROSION PROPERTIES OF BASALT FIBER REINFORCED CONCRETE

A Thesis

Presented in Partial Fulfillment of the Requirements for the

Degree of Master of Science

with a

Major in Civil Engineering

in the

College of Graduate Studies

University of Idaho

by

Kevin Ramirez

Major Professor: Ahmed Ibrahim, Ph.D.

Committee Members: Richard Nielsen, Ph.D., Emad Kassem, Ph.D.

Department Chair: Patricia J. S. Colberg, Ph.D.

December 2019

AUTHORIZATION TO SUBMIT THESIS

This thesis of Kevin Ramirez, submitted for the degree of Master of Science with a Major in Civil Engineering and titled "**Fresh, Mechanical, Durability and Corrosion Properties of Basalt Fiber Reinforced Concrete**," has been reviewed in final form. Permission, as indicated by the signatures and dates below, is now granted to submit final copies to the College of Graduate Studies for approval.

Major Professor: _____ Date: _____
Ahmed Ibrahim, Ph.D.

Committee Members: _____ Date: _____
Richard Nielsen, Ph.D.

_____ Date: _____
Emad Kassem, Ph.D.

Department Chair: _____ Date: _____
Patricia J. S. Colberg, Ph.D.

ABSTRACT

The main goal of this study is to investigate the effects of using basalt fibers on the fresh, mechanical, durability and corrosion properties of basalt fiber reinforced concrete (BFRC). The study is performed with varying basalt fiber volumes of 0%, 0.15%, 0.30%, 0.45% and 0.50% by total concrete volume; utilizing two different water/cement (w/c) ratios of 0.35 and 0.40. The results were compared to conventional concrete as well as steel fiber reinforced concrete (SFRC). The first part of the experimental program, consisted of 14 different concrete mixtures that have been cast using conventional Portland cement with a design compressive strength of 5,075 psi at 28 days (typical strength for slabs and similar applications in which fiber reinforced concrete (FRC) may be used). The second part of the experimental program investigated the effects of basalt fibers on corrosion rates and corrosion potential for steel reinforcement embedded in mortar mixtures. The first experimental program included fresh, mechanical and durability properties of the developed concrete mixtures. The fresh properties included slump and unit weight; mechanical properties included compressive strength, tensile strength, flexural strength and average residual strength; durability properties included unrestrained drying shrinkage and chloride ion penetrability evaluation. The second experimental program investigated the effects of basalt fibers on corrosion properties of steel reinforcement embedded in mortar by performing a rapid macrocell corrosion evaluation test.

It is concluded that the use of basalt fibers reduces slump values as fiber volume increases; however with the use of the right amount of High Range Water Admixture (HRWA), slump target values can be achieved. Results indicate that the use of basalt fibers improves tensile, flexural, and average residual strength properties as fiber volume increase; up to 28.92% for tensile strength and 45.86% for flexural strength. Results also suggest that the use of basalt fibers may decrease compressive strength at 28 days. Durability properties are also improved with the addition of basalt fibers as fiber volume increases. It is suggested to use a fiber volume of 0.30% to optimize overall mechanical and durability properties of the mixtures. On the other hand, results suggest that the use of basalt fibers may increase corrosion rates and accelerate the time of corrosion of steel reinforcement embedded in mortar. Therefore, is not suggested to be used for such applications.

ACKNOWLEDGEMENTS

To my advisor, Dr. Ahmed Ibrahim, I am grateful for the motivation, support, and academic excellence he provided me throughout my thesis and graduate studies. Working with him was an excellent opportunity of learning experience in an engineering practice sense as well as daily life advice. The patience he had for explaining difficult concepts related to this research is greatly appreciated. Without his help and continuous support this work would not have been possible. My sincere and profound thanks are due to Dr. Richard Nielsen and Dr. Emad Kassem for serving as members of my thesis reviewing committee.

I would also like to thank Olaniyi Arowojulu for the help provided with mixing and testing of the specimens and the guidance provided throughout the analysis portion of testing. Also, special thanks to Don Parks for his technical support throughout the testing. This work would not have been possible without their support as well.

I wish to express my gratitude and sincere appreciation to Pre-Mix Concrete Plant in Pullman, Washington for their generous support by donating all the materials required for concrete mixing. Without the help from Jesse Espy, manager at the Pre-Mix Concrete Plant, and the rest of their team this testing would not have been possible.

My huge appreciation to the Civil and Environmental Engineering Department at the University of Idaho for providing the necessary materials and financial support for the machines and materials required for this research. Acknowledgement is also due to the University of Idaho for the support given to this research through its facilities and for granting me the opportunity to pursue my graduate studies with financial support. I am blessed to have the wonderful opportunity to call Moscow, Idaho my home the past 6 years of my life.

DEDICATION

This work is dedicated to my father Celso Victor Ramirez, my mother Anastacia Ramirez, my brother Marvin Victor Ramirez, and all my friends here in Moscow, Idaho and all over the country for their constant guidance, encouragement and invaluable support throughout my studies. Without their moral support, this would not have been possible.

TABLE OF CONTENTS

LIST OF TABLES

LIST OF FIGURES

CHAPTER 1: INTRODUCTION

1.1 PROBLEM STATEMENT

Concrete is a composite material with high compressive strength but relatively low tensile strength and a low energy absorption capacity. Implementing fibers to a concrete mixture, in general, improves mechanical properties such as tensile, flexural, and improved toughness strength as well as reducing the brittleness of the concrete. The American Concrete Institute (ACI) defines Fiber-Reinforced Concrete (FRC) as concrete made primarily of hydraulic cements, aggregates, and discrete reinforcing fibers [1]. There are various commercially available fibers for use such as steel, glass, synthetic and natural materials. Steel fibers are the most common type of fibers being utilized (50% of the total used fibers), followed by polypropylene (PP) fibers (20% of total used fibers), glass fibers (5% of total used fibers) and lastly other types of fibers (25% of total used fibers) [2]. The increase in development of a durable and sustainable concrete has attracted major focus in the industrial and academic world to investigate the benefits of different types of fibers.

A relatively new type of fiber that has been suggested for use in FRC are basalt fibers. These fibers are an inorganic material produced from volcanic rock called basalt. The production of basalt fibers does not create any environmental waste, is nontoxic and requires less energy to produce when compared to glass or carbon fibers. Basalt fibers exhibit excellent structural properties such as high tensile strength, high thermal stability, light weight, non-corrosive and good chemical resistance, which makes it a potential alternative to common FRC fiber types.

The research reported in the published literature is promising, although limited and lack information about the implementation of basalt fibers in concrete. Generally, it has been found that basalt fibers increase the splitting tensile, flexural strength and toughness of concrete, but do not have a significant effect on the compressive strength. The addition of basalt fibers may also have a negative effect on the workability of the concrete which may limit the application of the fibers. Furthermore, the published research provides only limited data on the post-cracking and durability characteristics of BFRC. Therefore, to promote the use of basalt fibers,

research in BFRC mixtures is needed to further understand the benefits of implementing basalt fibers into concrete.

1.2 OBJECTIVE OF RESEARCH

This research presents a comprehensive study to develop and assess BFRCs for a typical structural application by studying the effects on the fresh and hardened properties of the developed mixtures. This can be achieved by preparing various BFRC mixtures with varying fiber dosages and compare their fresh properties, mechanical properties, durability properties and corrosive properties with control samples and steel fiber reinforced concrete (SFRC) samples. The fresh properties include slump and concrete unit weight. The mechanical properties include compressive strength, tensile strength, flexural strength and average residual strength at different ages. Durability properties include unrestrained drying shrinkage and chloride ion penetrability evaluation. Corrosion properties include corrosion rate and corrosion potential.

1.3 THESIS OUTLINE

The thesis is divided into two parts; the first part (Chapters 1 to 4) provides an introduction on the research being conducted as well as an introduction into fiber characteristics that affect FRC properties and presents the evaluation and analysis for the concrete mixtures developed in this research.

The second part (Chapter 5) provides a guideline to perform a rapid macrocell corrosion test and presents the evaluation and analysis for the mortar mixtures developed in this research.

Chapter 2: "LITERATURE REVIEW": This chapter summarizes relevant previous and existing research conducted on BFRC and FRC.

Chapter 3: "EXPERIMENTAL PROGRAM": This chapter covers the experimental plan and setup for the concrete mixtures along with the materials used and their properties. It also provides proportions of the concrete mixtures used for this study as well as the standards and testing procedures followed.

Chapter 4: “EXPERIMENTAL RESULTS AND DISCUSSION”: This chapter describes all the test results for the concrete mixtures; fresh, mechanical and durability properties studied in this research.

Chapter 5: “RAPID MACROCELL CORROSION EVALUATION”: This chapter presents the experimental evaluation of a corrosion protection system by performing a rapid macrocell test. The chapter introduces the purpose, test set-up and presents the test results for all mortar mixtures studied in this research.

Chapter 6: “CONCLUSIONS AND RECOMMENDATIONS”: This chapter presents the conclusions drawn from Chapter 4 and 5. Also, recommendations are provided in this chapter for future research.

CHAPTER 2: LITERATURE REVIEW

2.1 INTRODUCTION

The addition of fibers to concrete in order to improve mechanical properties such as tensile strength, flexural strength and post-cracking behavior has been investigated and used for decades [3, 4, 5]. Fibers made from steel, polypropylene, and glass are currently the most common fiber types used to produce fiber reinforced concrete. However, these type of fibers may exhibit weight problems, corrosion, chemical durability, fatigue, and increased cost in many applications. This has led the industry to focus on the development and investigation of other types of fibers as alternatives for reinforcement in polymer composites. From the various fibers available, basalt fibers have become one of the main focuses for research.

Basalt fibers are an inorganic material produced from volcanic rock called basalt. Basalt rock originates from volcanic magma and flood volcanoes which is then solidified in the open air. Due to the nature of basalt rock, its chemical composition can vary depending on the geographical location and conditions of source [6, 7]. The chemical structure of basalt rock is nearly related to glass with the most important components being: SiO_2, Al_2O_3, CaO, MgO, Fe_2O_3 and FeO [8, 9, 10]. Due to the abundant supply of basalt rock available and recent development in fiber production technology; basalt fiber displays significant potential and is considered as a viable alternative to traditional fibers by the composite industry [11, 12].

The inclusion of basalt fibers in FRC is a relatively recent practice so it is important to understand the effects BF have on the fresh, hardened and durability properties of the concrete in order to achieve a workable yet durable concrete. Basalt fibers have shown to have excellent characteristics such as high tensile strength, high heat resistance, high thermal stability, good chemical resistance, and relatively low production cost [11, 12]. Previous studies have found that in proper proportions, basalt fibers have shown to improve mechanical properties. Specifically, Patil et. al. [13] found that a fiber percentage of 0.50% per volume produced the highest compressive and flexural strengths among the three fibers tested (basalt, glass and steel) where BFRC obtained the highest strengths. Similarly, a study done by Yakhlaf et. al. [14] showed that a fiber dosage of 0.30% per volume provided an optimal concrete mixture. While the mechanical properties tend to increase due to the addition of basalt fibers, studies

have shown that the slump of concrete decreases. A study done by Jiang et. al. [15] observed the effects of basalt fiber on the workability of BFRC containing different aspect ratio fibers and different fiber proportions by total volume of concrete. Results demonstrated that the increase in fiber volume decreased the slump of the concrete. Kirthika et. al [16] conducted a similar study utilizing different fiber volumes where the results also displayed a reduction in workability with the increase in fiber content. The main reason of reduction in slump is due to the increase in surface area of the fiber which causes concrete to agglomerate around the fibers. In addition to the coarse aggregate, the mortar must also coat the fibers and so if the mortar fraction is insufficient then a reduction in slump will be observed. In order to increase the slump of the concrete, additives such as plasticizers must be introduced into the mix. It should be noted that slump loss does not necessarily mean that there is a corresponding loss of workability, especially when vibration methods are used during placement.

The durability properties of the concrete have also shown to be affected by the addition of BF into concrete mixtures. A study done by Singh et. al. [17], investigated the durability of BFRC in chemical solutions, carbonation, rapid chloride penetration (RCPT) and fire. The study showed that BFRC performed better than normal concrete. BFRC displayed significantly less carbonation, whereas normal concrete showed increased ion permeability at 56 days.

In summary, the addition of BF tends to decrease workability, slump, of concrete and has shown to have little to no effect in improving compressive strength but has shown to improve tensile and flexural strengths. Previous investigations have conducted research mainly focusing on the effects of the mechanical properties but have provided only limited data on the effects of the post-cracking and durability properties of the concrete.

2.2 DEVELOPMENT OF FIBER REINFORCED CONCRETE

The use of fibers in building materials can date back to ancient times. The implementation of straw fibers to sun-dried mud bricks was used by ancient Egyptians to improve the behavior of the material. This concept of using fibers intuitively created a composite material with an improved performance, in this case preventing cracking [18]. In modern times, the concept of fiber reinforcement can date back to the early 1900’s where brittle cement-paste was reinforced with asbestos fibers [19]. The fibers improved the matrix structure of the

cementitious material, but health issues associated with the fiber required the industry to investigate different fiber materials. This led to alternative fiber types to be introduced throughout the 1960s and 1970s giving rise to the development of composite materials.

Modern development of fiber reinforced concrete started with scientifically based studies done by J.P. Romuldi, J.A. Mandel and G.P. Batson [20, 21] in the years of 1963 and 1964. These studies brought awareness of the improvement in fracture resistance of the composite by the addition of steel fibers. This created a starting point for further research and development of fibre-reinforced construction materials. In this day and age, there is a multitude of fiber types and fiber materials in the market with new materials being continuously introduced as new discoveries and new applications are identified. The introduction of new fibers can be attributed to the progress made in fiber technology as well as the intensive research studies conducted in order to better understand the effects of fibers. Studies have been conducted to investigate the effects of implementing fibers and have shown FRC to be primarily dependent on the properties of the fibers and the dispersion of the fibers in the concrete matrix [22, 23, 24, 25]. The main characteristics to consider are the fiber material, fiber geometry, fiber distribution/orientation and fiber concentration [26, 27, 28, 29].

2.2.1 Fiber Materials

The properties of the fiber material being used are crucial when developing a FRC mix. Properties such as: modulus of elasticity, tensile strength, and strain at failure are fiber properties to take into account. A list of typical commercially available fibers and their properties can be seen in Table 2-1.

Table 2-1: Typical Fiber Materials

Fiber Type	Specific Gravity (g/cm^3)	Tensile Strength (MPa)	Young's Modulus (GPa)	Elongation at Break (%)
Steel	7.86	280-2800	210	0.5-35
E-Glass	2.57	3450	72.5	2.5
AR-Glass	2.68	3700	74	2.5
Carbon	1.70	3700	250	1.2
Polypropylene	0.91	400	1-8	25
Polyethylene	0.95	2588	117	10
Basalt	2.6	1000	7.6	2.6
Cellulose	1.5	300-1000	10-50	20

From the current commercially available fiber materials, four main types of FRC have been established:

1) SFRC- Steel Fiber Reinforced Concrete
2) GFRC- Glass Fiber Reinforced Concrete
3) SNFRC- Synthetic Fiber Reinforced Concrete
4) NFRC- Natural Fiber Reinforced Concrete

From the literature, it has been reported that steel fibers are the most common type of fibers used due to the high modulus of elasticity of the material and the improved mechanical properties, mainly toughness, it provides to the composite [2, 30, 31, 32, 33, 34, 35]. Fibers with high modulus have shown to simultaneously improve both flexural and impact resistance. On the other hand, fibers with low modulus, such as polypropylene, have shown to improve toughness and early age cracking, but do not contribute much to concrete flexural strength.

2.2.1.1 Steel Fibers

Historically, steel has been used as the material for reinforcement in concrete. Due to the high elastic modulus of the material and intensive research conducted, steel is currently the most used type of fiber in the industry. Figure 2-1 shows a typical type of steel fiber used in SFRC.

Figure 2-1: Steel Fibers (Authors Figure)

Steel fibers are generally produced from carbon steel and stainless steel and can be described as “discrete, short lengths of steel having an aspect ratio from about 20 to 100, with any of several cross-sections, and that are sufficiently small to be randomly dispersed in an unhardened concrete mixture using usual mixing procedures” ACI 544.1R-96 [1]. Steel fibers are classified into five categories as specified by ASTM A820/ A820 M-16 [36]:

- Type I: Cold-Drawn Wire
- Type II: Cut Sheet
- Type III: Melt-Extracted
- Type IV: Mill Cut
- Type V: Modified Cold-Drawn Wire

Steel fibers have desirable material properties such as a relatively high strength and modulus of elasticity. Typically, steel-fibers are used in volumes ranging from 0.25% to 2% and have shown to improve tensile and flexural strengths at higher volumes. Utilizing volumes higher than 2% has shown to reduce workability and create problems with uniform dispersion of the fibers in the cementitious matrix. In order to enhance the workability and stability of FRC,

adding chemical admixtures, such as superplasticizers, to the mix have shown to be effective as well as increasing fine materials and cement content.

2.2.1.2 Glass Fibers

Glass fibers are another type of fiber widely used in FRC, making up around 5% of the total fiber consumption. The use of glass as a construction material was available since the 1940's, with materials such as borosilicate glass (E-glass) and soda-lime-silica glass (A-glass) fibers being available [37]. Limitations on the use of glass fibers were primarily due to the low alkali resistance of the materials, as these type of fibers deteriorated rapidly within the highly alkaline environment of the cementitious matrix [37].

Figure 2-2: Glass Fibers (AR-Glass) [Womersleys.co.uk]

It was not until around the mid-1960's when a solution to the low alkali resistance of the fibers was implemented, the addition of zirconium dioxide into the production of the fibers. The addition of such mineral improved the glass fibers by creating an alkali resistance fiber type, currently known as Alkaline Resistant glass (AR-glass) fibers [12, 37, 38] which can be seen in Figure 2-2.

There is a wide variety of glass fiber types available, generally falling into two categories. Low-cost general-purpose fibers (such as E-glass) and special-purpose fibers (such as ECR-glass) [12, 39]. Table 2-2 shows different types of commercially available glass fibers and their mechanical properties.

Table 2-2: Glass Fiber Types

Fiber Type	Specific Gravity (g/cm^3)	Tensile Strength (MPa)	Young's Modulus (GPa)	Elongation at Break (%)
General Purpose Fibers				
Boron-Containing E-Glass	2.54-2.55	3100-3800	76-78	4.5-4.9
Boron-Free E-Glass	2.62	3100-3800	80-81	4.6
Special-Purpose Fibers				
ECR-Glass	2.66-2.68	3100-3800	80-81	4.5-4.9
D-Glass	2.16	2410	-	-
S-Glass	2.48-2.49	4380-4590	88-91	5.4-5.8
Silica/quartz	2.15	3400	69	5

Currently, the main industrial application of glass fibers is primarily in exterior building facade panels and as architectural precast concrete. There are two main production techniques of GFRC, referred to as spray-up and pre-mix, which can be seen in Figure 2-3.

Spray-up technique is similar to shotcrete in that the fluid concrete mixture, without the fibers, is sprayed into the formwork with the use of a spray gun. This process produces the concrete separately and mixes the fibers only at the jet of the spray gun. Glass fibers are fed off of a spool in a continuous thread into the gun, where blades cut the fibers just before being sprayed. This technique allows for longer fibers, around 1.5 in., to be used in the mix where it is typically applied in two layers. The first layer is the face coat, essentially just a thin layer without fibers often only about 3-4mm thick; the second layer is where the fiber is introduced. This technique allows for a built-up of layers of about 4-6mm thickness with each pass ensuring structural integrity of the fibers within the matrix.

Figure 2-3: GFRC Production Techniques [Alibaba.com]

The second type of GFRC production type is the premix method. This method is typical in FRC as the cement is produced first and fibers are added to the mix in the fresh state. Fibers are weighed beforehand where conventional mixing techniques for concrete only allow around 2%, by volume, addition of fibers with typical glass fiber lengths around 6-12mm. As with any type of fiber, the addition of higher volumes of fibers or longer types of fibers are limited due to the reduction in workability that would be produced.

2.2.1.3 Synthetic Fibers

Synthetic fibers are another widely used type of fiber used in FRC. Synthetic fibers are man-made fibers resulting from intensive research and development in the petrochemical and textile industries [5, 40, 41, 42]. Typical synthetic fibers for SNFRC and their properties can be seen in Table 2-3.

Table 2-3: Synthetic Fiber Types

Fiber Type	Specific Gravity (g/cm^3)	Tensile Strength (MPa)	Young's Modulus (GPa)	Elongation at Break (%)
Acrylic	1.18	200-1000	17-19	28-50
Aramid	1.44	2000-3100	62-120	2-3.5
Carbon	1.90	1800-2600	230-380	0.5-1.5
Nylon	1.14	1000	5.2	20
Polyester	1.38	280-1200	10-18	10-50
Polyethylene	0.96	80-600	5	12-100
Polypropylene	0.90	450-700	3.5-5.2	6-15

From the various synthetic fibers types available, polypropylene (PP) fibers have been the most widely used in FRC to enhance the toughness and shrinkage control of the concrete [41]. PP fibers have unique properties that make them favorable in FRC usage, such as:

- Chemically inert
- High Melting Point
- Hydrophobic
- Lightweight

Figure 2-4: Polypropylene (PP) Fibers [Jeetmull Jaichandlall Madras Pvt. Ltd.]

Polypropylene (PP) fibers, shown in Figure 2-4, are currently manufactured in a variety of geometries and configurations; produced by drawing the synthetic polymer into continuous cylindrical monofilaments that can be chopped to specific lengths or cut as films or tapes, which are then produced into fine fibers. PP fibers can be produced as monofilaments, collated fibrillated fibre bundles and continuous films [5, 42].

2.2.1.4 Natural Fibers

Natural fibers are the last type of fibers used in FRC. Natural fibers have been used for decades and can date back to ancient Egyptians who implemented straw fibers to sun-dried mud bricks to improve the behavior of the material. The main advantage of using natural fibers is the availability of the materials, low cost of production, non-abrasive characteristics and are a renewable material [5, 43, 44]. Through the advancement in fiber technology, a wide variety of natural fibers have become available to produce NFRC; Table 2-4 shows a list of typical natural fibers available.

Table 2-4: Natural Fiber Types

Fiber Type	Specific Gravity (g/cm^3)	Tensile Strength (MPa)	Young's Modulus (GPa)	Elongation at Break (%)
Basalt	2.63-2.8	4100-4800	90-110	3.1-3.2
Wood Cellulose	1.50	350-2000	62-120	2-3.5
Sisal	-	280-600	230-380	0.5-1.5
Coconut	1.12-1.15	120-200	5.2	20
Bamboo	1.50	350-500	10-18	10-50
Jute	1.02-1.04	250-350	5.0	12-100
Elephant Grass	-	180	3.5-5.2	6-15

Natural fibers tend to have lower tensile strength and modulus, as can be seen from the Table 2-4, which limits their use in FRC. Unprocessed natural fibers have been used to make thin sheets for walls and roofs and have displayed improved mechanical properties [5, 44]. Although natural fibers have shown to improve mechanical properties, the main disadvantage

is their low tensile strength, durability issues, inconsistency in properties and poor adherence to the concrete matrix [45].

As a result, natural fibers such as wood cellulose fibers and basalt fibers have been able to be processed in order to achieve higher tensile strengths and more consistency in fiber properties. Processed natural fibers highly depend on the method of production. In the case of wood cellulose fibers, the method by which the fibers are extracted and the refining process involved greatly influence the properties of the material. As for basalt fibers, it is the chemical composition of the rock before production that dictates their properties [9, 10, 12]. Typical manufacturing processes for basalt and wood cellulose fibers can be seen in Figures 2-5 and Figure 2-7, respectively.

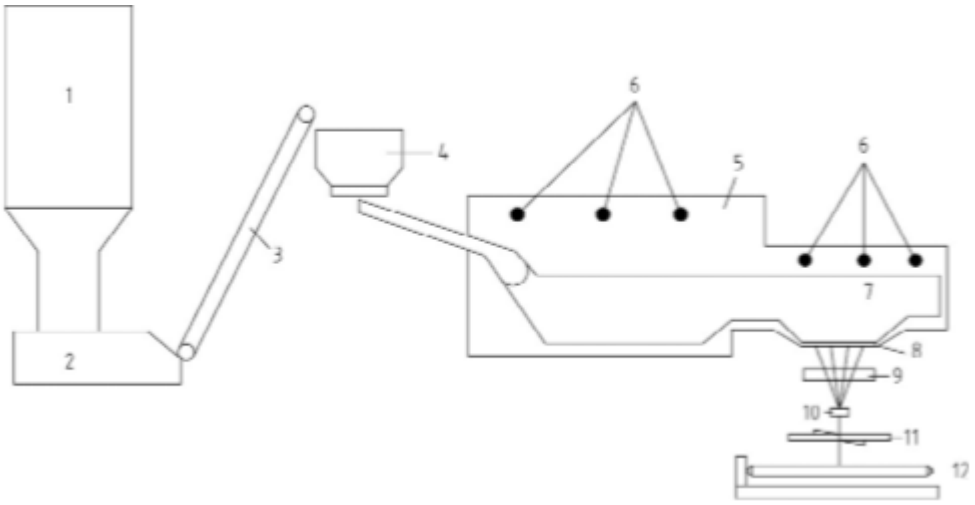

Figure 2-5: Basalt Fiber Production Schematic by Li Zongwen et. al [97]

As can be seen from Figure 2-5, the process for basalt fiber production is simple and is as follows:

1) Batch Silos: Raw material is supplied
2) Loading Station: Material is weighed and mixed
3) Pneumatic Transport: Material is transported
4) Batch Box: Batch charging station
5) Melting Furnace: Initial melt zone
6) Melting Furnace Continued: Secondary heat zone with precise temperature control
7) Filament Forming: Continuous filament-forming bushings

8) Sizing Applicator: Sizing application
9) Draw Plate Feeder: Strand formation station
10) Buncher: Material strands twisted
11) Fiber Tensioning Station: Fibers are tensioned
12) Automated Winder: Winding station

This process requires only the raw material, basalt rock, making the process of production inexpensive and readily available. Figure 2-6 shows typical basalt fibers produced.

Figure 2-6: Basalt Fibers (Authors Figure)

The production of wood cellulose fibers is somewhat more complex when compared to the production of basalt fibers. The process for extracting the fibers from wood is called pulping. Pulping can be done mechanically, chemically or a combination of both [46, 47, 48]. Chemical pulping process is the most common method due to the effectiveness of reducing the lignin, there are two main types of chemical pulping methods: The kraft or sulphate (alkaline) process and the sulphite (acidic) process. The chemical pulping process is shown in Figure 2-7.

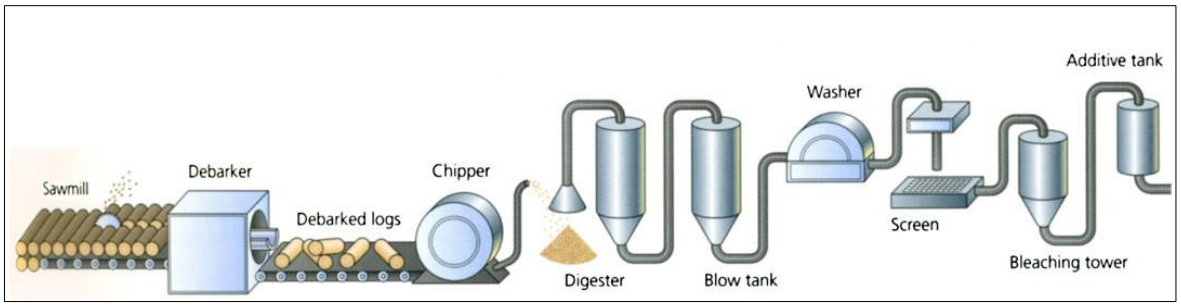

Figure 2-7: Wood Cellulose Fiber Production Schematic [csun.edu]

The objective of chemical pulping process is to remove enough lignin to separate cellulosic fibers one from another [47]. This process produces a pulp suitable enough for manufacture of paper and other related products [48]. The following list displays the several stages taken for production:

1) Material: Natural wood material is collected and debarked
2) Chipping: Wood is made into chips
3) Digesting: Pulping process
4) Washing: Washing of pulp product to recover chemicals
5) Screening: Removal of impurities (uncooked chips)
6) Bleaching: Pulp is bleached to attain a whiter (brighter) material for use
7) Additives: Chemical additives or fillers may be added to improve certain qualities

The manufacturing process is basically a two-step process in which raw material is converted into pulp and then converted into paper and other related products [48]. The following figure shows typical wood cellulose fibers produced.

Figure 2-8: Wood Cellulose Fibers [Wuxi Green Construction Technology Co., Ltd]

2.2.2 Fiber Geometry

Fiber geometry is another important fiber characteristic to take into account. This includes properties such as: Fiber length, diameter, aspect ratio (L/D), cross section shape and presence or absence of hooks at the ends of the fibers [1, 12, 17, 26, 49, 50, 51]. Fiber lengths may range from 6mm to 150mm (0.25in. to 6in.) and thicknesses ranging from 0.005mm to 0.75mm. (0.0002in. to 0.03in.). While fiber shapes may be round, flat, crimped, twisted or deformed depending on the applications of the fibers [5, 19, 26, 49, 50, 52]. Typical fiber cross-sectional shapes and geometries vary from circular and quadratic shapes to octagon and irregular shapes.

Literature has shown that longer fibers tends to bridge cracks better and improved flexural strength can be obtained by increasing the aspect ratio [26, 52, 53]. However, utilizing a high aspect ratio fiber increases the potential for balling of the fibers creating further workability problems within the mix. Micro fibers, on the other hand, have shown to be most effective at increasing performance parameters, such as plastic shrinkage, during early stages of crack

formation. Figure 2-9 shows the different levels of micro and macro cracks developed and how short and longer fibers attend to each type of crack.

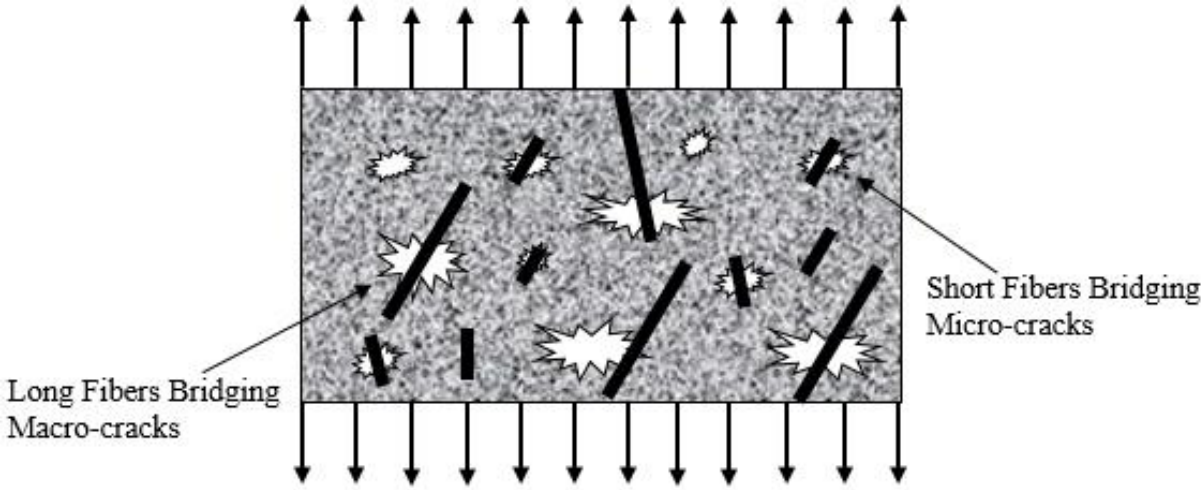

Figure 2-9: Long and Short Fibers Bridging Micro and Macro-cracks (Authors Figure)

Other fiber characteristics such as the fiber shape (straight or deformed) and geometry modifications such as: Indentation, crimping, and hooking the ends; play an important role in the fiber/matrix interface bonding parameter [27, 54, 55, 56], see reference by Ingemar Löfgren (2005) [60] for further fiber shape characteristics.

The fiber/matrix bond is crucial to the performance of the composite and is a result of several types of fiber/matrix interactions which ultimately affects the energy absorption characteristic of the fibers as stated by Singh et. al [55]. The fiber/matrix interaction can be explained as follows: Failure of bond matrix occurs and fibers bridge the preceding cracks. The processes that occur within this interaction can be seen in Figure 2-10 and is as follows:

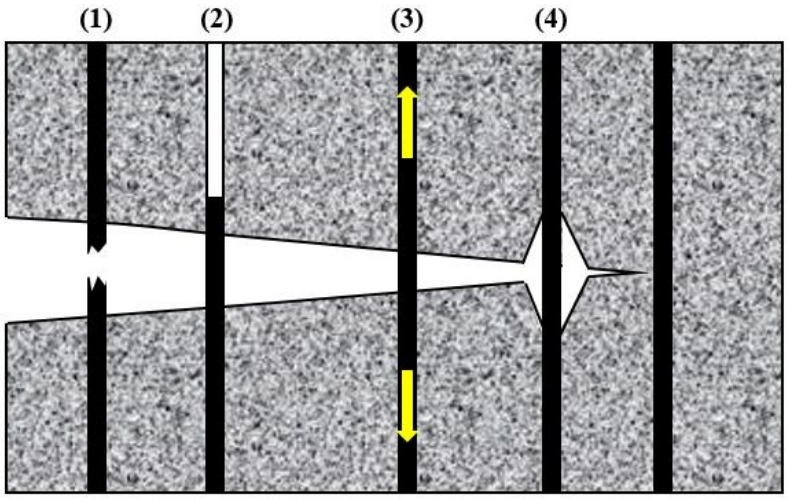

Figure 2-10: Energy Absorption Mechanism in FRC (Modified from original figure by Singh et. al.) [55]

1) Fiber fails (ruptures)
2) Fiber pullout (sliding)
3) Fiber bridging
4) Fiber/Matrix debonding

The pullout fiber mechanism is further explained by Halvaei et. al. [27] as being a series of two different parts: The breaking of chemical bonds and mechanical interlocking. Chemical treatments on the fibers have shown to impact the chemical bond interface of the fiber/matrix [12, 56, 57]. In a study done by Soulioti et. al. [57] steel fibers chemically treated with zinc phosphate showed an improved fiber/matrix interface, which lead to an increased fiber pullout peak load. The fiber pullout strength is the energy required to completely pull-out a fiber from the cementitious matrix. Research has also shown that mechanical interlocking is crucial for the effectiveness of fibers. Modifying the geometry of the fibers, such as hooking the ends, has shown increased pullout strength when compared to straight fibres due to the mechanical anchorage created by the deformed shape [54, 57, 58, 59].

2.2.3 Fiber Distribution & Orientation

Fiber distribution/orientation is another fiber characteristic that affects the effectiveness of the fibers in the cement matrix. Fibers may be dispersed in a direct or a random orientation in the cementitious matrix and is generally assumed a uniform (i.e., homogeneous and isotropic) distribution of fibers. A direct orientation is characterized as a one-dimensional (1-D) system

which is realized mainly by using continuous filaments, whereas, random orientation may be described as two-dimensional (2-D) and three-dimensional (3-D) systems. Further insight into orientation systems is best described by Ingemar Löfgren (2005) [60].

Literature has shown that the more the aligned fibers are into the direction of the tensile stress, the more number of fibers per unit cross sectional area, the more effective the fibers will be [26, 60, 61, 62, 63]. Figure 2-11 displays the importance of fiber angle orientation.

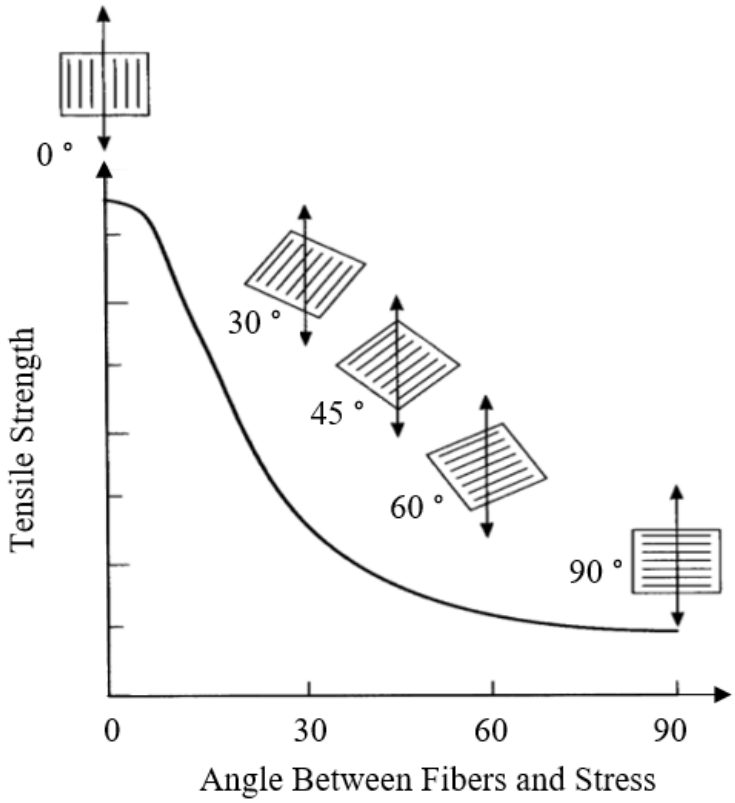

Figure 2-11: Fiber Angle Orientation Effect on Tensile Strength [Quora.com]

The effectiveness of fibers bridging cracks is related to the number of fibers per unit cross-sectional area, which can be computed with the following equation:

$$N_1 = \alpha \frac{V_f}{A_f} \quad (1)$$

Where:

N_1 = Number of fibers per unit area

V_f = Volume fraction of fibers in concrete

A_f = Cross-sectional area of a single fiber

α = Orientation factor

The orientation factor (α) is taken as follows (Ingemar Löfgren 2005):

	1-D	2-D	3-D
α Value	1	2/π	1/2

Research has shown that the following parameters also influence the distribution/orientation of the fibers: Fresh state properties, casting method, shape/dimension of the formwork, flowability characteristics, and the wall-effect of the formwork [26, 28, 61, 63, 64, 65]. A study done by Stähli et. al. [63] investigated the effects of flow properties on the behavior of fiber distribution/orientation.

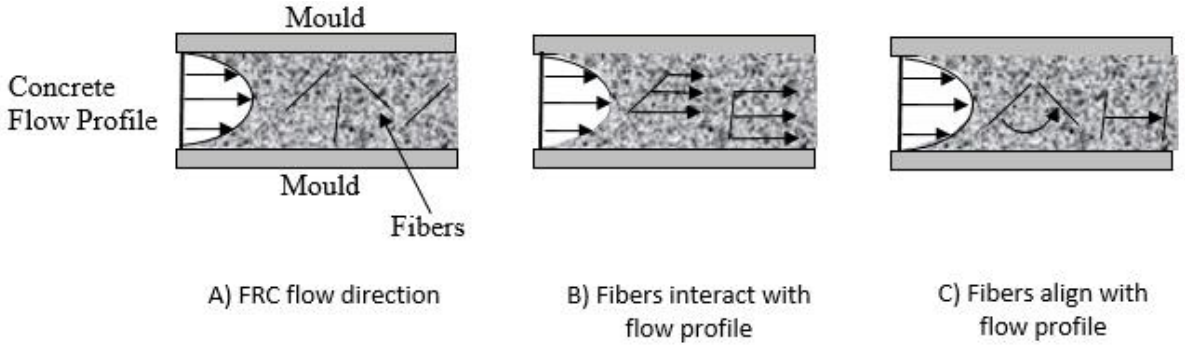

Figure 2-12: FRC Flow Profile (Modified from original figure by Stähli et. al.) [63]

The study found that fibers tend to align with the flow of the fresh concrete which was also influenced by the viscosity of the fresh concrete. An explanation to why this occurs may be due to the flow profile created when the concrete is cast, as shown in Figure 2-12. Along with flow profile, shape and dimensions of the formwork has shown to affect the distribution/orientation of the fibers as well.

Figure 2-13: Typical Standardized Formwork (Authors Figure)

Formwork usually entail standardized molds in academic research settings, as shown in Figure 2-13, but in actual construction these vary from slabs, beams, columns and many other type of shapes. A study done by Laranjeira et. al. [65] gives more insight into the influence the cross-section of typical formwork (rectangular, circular, and hollow) geometries have on fiber orientation.

The restriction of the fibers orientation alignment has typically been shown to be improved by restricting the formwork size, smaller size specimens displays a more effectively aligned fiber distribution [64]. The casting methods are still a topic of research, in terms of layer thickness, casting direction and forms of vibration. There are also numerous models to predict fiber orientation and the various parameters that affect the orientation and distribution of fibers within the mix.

2.2.4 Fiber Concentration

Fiber concentration is another fiber characteristic that affects the effectiveness of the fibers in the cement matrix. Fiber concentration refers to the amount of fibers in a cementitious mix and is measured as a percentage of the total volume of the composite (concrete and fibers). Fiber volume can be characterized into three groups [66]:

1. Low Fiber Volume (<1%)

2. Medium Fiber Volume (1-2%)
3. High Fiber Volume (>2%)

Low fiber volume is typically used to control plastic shrinkage, crack propagation control and crack widths reduction but displays no significant improvement in strength [14, 67, 68]. Medium fiber volume has shown to be applicable to supplement the main reinforcement in the member in order to provide improved mechanical properties such as toughness, and crack control. Medium fiber volumes are typically used in cast-in-place or precast FRC members [69, 70, 71, 72, 73, 74]. High fiber volumes are mainly used for structures that require improved toughness, enhanced ductility, and improved fracture energy [75, 76].

Although the fiber volume changes with the type of application, the main use of fibers is to improve the brittleness of the concrete, toughness, crack propagation and reduction in crack width. The use of fibers is not to replace the main reinforcement in the members, but rather enhance certain mechanical characteristics within the member utilizing the fibers as a bridging mechanism, see Figure 2-14.

Figure 2-14: (Left) Fiber Bridging, (Right) Typical FRC Cross-Section (Authors Figure)

The bridging mechanism of fibers is best utilized in preventing or controlling the propagation of cracks in the composite. Cracks in concrete is a multiscale process that starts at a micro scale and eventually propagate into a large macro crack. Crack development stages are best explained in more in-depth by Ingemar Löfgren (2005) [60].

The most important aspect of the inclusion of fibers is the improved toughness characteristics concrete attains. Toughness is a measure of the ability of concrete to absorb energy during deformation, which can be measured by the area under the stress-strain (load-deformation) diagram. An increase in toughness can be obtained by the addition of fibers and is related to the fiber volume utilized within the mix.

Plain concrete displays little to no energy absorption characteristics and as such, once concrete starts to crack, the member tends to fail and is no longer able to withstand stresses past post-cracking. FRC, on the other hand, is able to sustain loads at strains much greater than those at which first crack propagates within the matrix. This in return significantly increases the post-cracking ductility of the material and is proportional to the fiber volume used.

The use of too much fibers per volume does arise, especially when using 2% and higher fiber percentages per volume. This is a main issue in UHPC (Ultra High Performance Concrete), where not only the fiber volumes tend to be as high as 5% per volume, but the w/c ratios can be as low as 0.25 [77]. The combination of a low w/c ratio and high fiber volume can result in fibers not being optimized and resulting in fiber balling problems.

In order to address this problem, the use of chemical admixtures such as HRWRA (High Range Water Reducing Admixtures) or superplasticizers is essential, in order to provide workable concrete without compromising the strength. It is important to utilize a proper dosage of chemical admixtures in order to prevent segregation of the fine materials or bleeding within the mix. References such as [78, 79, 80] and many others provide information on the applications and specification on various chemical admixtures available.

CHAPTER 3: EXPERIMENTAL PROGRAM

3.1 INTRODUCTION

In this chapter, the details of the experimental program conducted at the "Buchanan Engineering Laboratory" at the University of Idaho (UI) are discussed and reported. The concrete batch matrix can be seen in Table 3-1, material properties in Table 3-2, concrete mix design in Table 3-3 and the tests performed can be seen in Table 3-4. The aim of the tests is to study the fresh, mechanical and durability properties of the concrete mixtures made with the inclusion of basalt fibers. The study was done with varying basalt fiber volumes of 0%, 0.15%, 0.30%, 0.45% and 0.50% by total concrete volume; utilizing two different water-to-cement ratios (w/c) of (0.35, 0.40) and comparing them to conventional concrete as well as SFRC samples utilizing 0.30% and 0.50% by total concrete volume. All of the test specimens had the necessary equipment and instruments to measure and record data from the experiments.

3.2 TEST OBJECTIVES

The aim of this project is to investigate the effects of basalt fiber on the fresh, mechanical, and durability properties of concrete by conducting experimental testing to evaluate the effects of different fiber volumes, using two water-to-cement ratios. Also, a comparison between steel and basalt fibers have been performed to asses which of the two fibers provides a better overall performance.

A total of 14 concrete mixtures were designed based on typical mixtures used by ITD (Idaho Transportation Department) for bridge constructions, which can be seen in Table 3-3. Fiber volume guidelines were taken from literature as well as ACI 544.1R-96 Report on Fiber Reinforced Concrete [1] and ACI 544.4R-18 Design Considerations for Steel Fiber Reinforced Concrete [81]. Fiber volumes were not to surpass 1% by volume as this research does not aim to investigate high fiber volumes and is aimed more towards typical fiber volumes used (<1%). The dosages of superplasticizer were adjusted for each fiber volume content to achieve the desired slump of 6in. ± 2in. where superplasticizer dosage guideline was taken from [17, 78, 79, 80] and adjusted to the appropriate mix design volume of 1.7 ft^3. Slump-flow test and fresh density test were performed to evaluate the fresh properties of all

mixtures. Furthermore, the mechanical properties such as compressive strengths at 7, 14, and 28 days, tensile strength at 28 day, flexural strength at 28 days, residual strength at 28 days, and unrestrained shrinkage up to 91 days were also investigated. In order to investigate durability properties, surface resistivity test were performed at 28 days. All mixtures were labeled according to the group and volume percentage. The mixtures were divided into two groups; Group I consisted of a control mixture, BFRC, and SFRC mixtures with w/c ratio of 0.35, labeled (MA= Mixture A), and Group II consisted of the same mix design, but with a w/c ratio of 0.40, labeled (MB= Mixture B). Table 3-1 shows the mix design batch matrix utilized for this experimental program.

Table 3-1: Concrete Batch Matrix

Group (W/C Ratio)	**Concrete Mix**	**Basalt Fiber (Kg/m^3)**	**Steel Fiber (Kg/m^3)**
Group I (0.35)	MA (Control)	None	None
	MA (15)	4.05	None
	MA (30)	8.10	None
	MA (45)	10.80	None
	MA (50)	13.49	None
	MA (Steel 30)	None	23.54
	MA (Steel 50)	None	39.23
Group II (0.40)	MB (Control)	None	None
	MB (15)	4.05	None
	MB (30)	8.10	None
	MB (45)	10.80	None
	MB (50)	13.49	None
	MB (Steel 30)	None	23.54
	MB (Steel 50)	None	39.23

3.3 MATERIALS

In the development of all mixtures, a Type I/II Portland cement with a specific gravity of 3.15 and conforming to the requirements of the ASTM C150, “Standard Specification for Portland Cement” [82] was used. Crushed basalt with a nominal particle size of 19mm (0.75in.) was used as coarse aggregate (CA). Natural sand was used as fine aggregate (FA). Moisture absorption and specific gravity for coarse and fine aggregate were determined in accordance to ASTM C127, “Standard Test Method for Relative Density (Specific Gravity) and Absorption of Coarse Aggregate” [83] and ASTM C128, “Standard Test Method for Relative Density (Specific Gravity) and Absorption of Fine Aggregate” [84], respectively. The relative specific gravity (SSD) and absorption of the coarse aggregate were 2.729 and 2.73%, respectively, whereas the fine aggregate had a relative specific gravity (SSD) of 2.683, absorption of 4.03%, and a fineness modulus of 2.93. A high range water reducing admixture (HRWA) utilizing Sika’s ‘ViscoCrete®4100’ confirming the requirements for ASTM C 494 Types A and F was also used in the concrete mixtures. The recommended dosages are between 325-780 mL/100kg (5-12 fl oz. /100 lbs) of cementitious materials. The basalt fiber and steel fiber were provided by Deutsche Basalt Faser GmbH, Germany, and Sika Corporation, USA, respectively. Figure 3-1 shows the basalt and steel fibers used in the mixtures. The material properties are listed in Table 3-2.

Table 3-2: Concrete Mixture Material Properties

Material	Properties
Portland Cement (C)	Relative Density: 3.15
Crushed Basalt Coarse Aggregate (CA)	Maximum Aggregate Size: 19mm (3/4”)
	Saturated Surface-Dry (SSD) Based Relative Density: 2.729
	Absorption: 2.73%
	Graded in Accordance with ASTM C 33 (19mm (3/4”))
Natural Sand (FA)	Relative Density: 2.683
	Absorption: 4.03%
	Fineness Modulus: 2.93
	Graded in Accordance with ASTM C 33
Basalt Fibers (BF)	Relative Density: 2.70
	Fiber Length: 24.13mm (0.950”)
	Diameter: 0.60mm (0.0235”)
	Aspect Ratio: 40
Steel Fiber (SF)	Relative Density: 7.85
	Fiber length: 38mm (1.5”)
	Diameter: 1.14mm (0.045”)
	Aspect Ratio: 34
	Tensile Strength: 966-1242 MPa (140-180 Ksi)
	Elastic Modulus: 205 GPa (29700 Ksi)
High-Range Water Reducing Admixture (HRWA) (Sika Viscocrete-4100)	Relative Density: 1.08
Normal Tap Water (W)	Density at 24°C (75.2 °F): 997.28 Kg/m^3 (62.3 lb/ft^3)

Figure 3-1: (Left) Basalt Fiber, (Right) Steel Fiber (SikaFiber Force XR)

3.4 PREPARATION OF SAMPLES & MIXING PROCEDURES

A rotatory drum mixer was used to mix all concrete materials in accordance with ASTM C 192 “Standard Practice for Making and Curing Concrete Test Specimens in the Laboratory” [85]. First, the coarse and fine aggregates were added to the rotating mixer and mixed for 30 seconds and the aggregates were brought to Saturated Surface Dry (SSD) conditions by adding a small amount of water. After the SSD aggregates were mixed for another 30 seconds, the cement was added to the mixer and continued to mix for another 30 seconds. Next, 60% of the water was poured over the mix, and the mixing continued for another 30 seconds. The HRWA, if included, was added to the remaining water which was added to the mix and allowed to mix for another 60 seconds. The fibers, if included, were then added to the mixer after stopping for 30 seconds in order to prevent the fibers from clumping together, fibers were added 50% at a time. Then the mixing was continued until the homogenous mixture was produced. Generally, the total time for mixing ranged from 10 to 15 minutes. The fresh properties were measured immediately after mixing. To ensure mixture homogeneity, mixing was resumed for the intervals between the two subsequent tests (slump flow and fresh density).

Table 3-3: Concrete Mix Design

	Control		BFRC								SFRC			
Material	MA (C)	MB (C)	MA (15)	MB (15)	MA (30)	MB (30)	MA (45)	MB (45)	MA (50)	MB (50)	MA (Steel 30)	MB (Steel 30)	MA (Steel 50)	MB (Steel 50)
Cement (Kg/m^3)	371	371	371	371	371	371	371	371	371	371	371	371	371	371
(lbs/yd^3)	1355	1355	1355	1355	1355	1355	1355	1355	1355	1355	1355	1355	1355	1355
C.A. (Kg/m^3)	985	985	985	985	985	985	985	985	985	985	985	985	985	985
(lbs/yd^3)	1660	1660	1660	1660	1660	1660	1660	1660	1660	1660	1660	1660	1660	1660
F.A. (Kg/m^3)	804	804	804	804	804	804	804	804	804	804	804	804	804	804
(lbs/yd^3)	1355	1355	1355	1355	1355	1355	1355	1355	1355	1355	1355	1355	1355	1355
Water (Kg/m^3)	130	148	130	148	130	148	130	148	130	148	130	148	130	148
(lbs/yd^3)	219	250	219	250	219	250	219	250	219	250	219	250	219	250
Fibers (Kg/m^3)	0.0	0.0	4.05	4.05	8.10	8.10	10.8	10.8	13.5	13.5	23.54	23.54	39.23	39.23
(lbs/yd^3)	0.0	0.0	6.83	6.83	13.7	13.7	18.2	18.2	22.7	22.7	39.68	39.68	66.12	66.12
HRWA (L/m^3)	0.0	0.0	0.60	0.50	0.60	0.50	0.60	0.50	0.62	0.62	1.04	0.73	0.83	0.52
(gal/yd^3)	0.0	0.0	0.12	0.10	0.12	0.10	0.12	0.10	0.13	0.13	0.21	0.147	0.167	0.105

Figure 3-2: Curing Room and Concrete Samples Being Cured in Water Tank

From each concrete mixture, a total of nine 100 x 200mm (4 x 8 in.) concrete cylinders, one 150 x 300mm (6 x 12 in.) concrete cylinder, and one 150 x 150 x 500mm (6 x 6 x 20 in.) concrete beam were prepared. The nine cylinders were used to measure the compressive strength at 7, 14, and 28 days; the 6 x 12 in. cylinder was used to measure the tensile strength at 28 days and the 6 x 6 x 20 in. beam was used to measure the flexural strength of the concrete at 28 days. All prepared concrete cylinders and prisms were covered and left in plastic molds undisturbed for 24 hours. Subsequently, they were unmolded and stored in 95% or higher humidity until the day of testing. All the moist-cured samples were tested within one hour after removal from curing room. Figure 3-2 shows concrete samples being cured in the curing room. An additional three 50 x 50 x 250mm (2 x 2 x10 in.) concrete prisms were also prepared from each concrete mixture in accordance with ASTM C 490 “Standard Practice for Use of Apparatus for The Determination of Length Change of Hardened Cement Paste, Mortar and Concrete” [86]. Samples were cast, covered, and kept undisturbed in the curing room for 24 hours. After unmolding, the specimens were kept in the curing room at 95% or higher

humidity for 7 days followed by air curing at room temperature, which can be seen in Figure 3-12. The mentioned samples are shown in Figure 3-3 after demolding and appropriate labeling.

Figure 3-3: Concrete Specimens

Additionally, three 50 x 50 x 300mm (2 x 2 x 12 in.) concrete prisms were also prepared from each concrete mixture to measure the average residual strength of the concrete at 28 days (Figure 3-4). Test specimens were mixed in accordance to ASTM C 192 “Practice for Making and Curing Concrete Test Specimens in the Laboratory” [85]. The test specimens were cast, covered, and kept undisturbed in the curing room for 24 hours. After unmolding, the specimens were kept in the curing room at 95% or higher humidity for 28 days. It should be noted that these specimens were prepared at a later time due to max capacity of the drum mixer (1.7 ft^3), which is why they do not appear in Figure 3-3.

Figure 3-4: ARS Beam Specimens

3.5 STANDARD TESTS AND TESTING PROCEDURES

The tests are performed in three stages; testing for fresh properties, mechanical properties testing and durability testing. First, the fresh properties of concrete mixtures were evaluated to ensure that the concrete met the desired mix design property (slump) and to evaluate concrete unit weight differences within each mix. Then, the mechanical properties (compressive strength, tensile strength, flexural strength and average residual strength) of all prepared concrete mixtures were evaluated. Finally, the durability of all concrete mixtures was assessed by measuring the unrestrained shrinkage and surface resistivity. The tests performed, the number specimens per test and the standard testing methods followed are presented in Table 3-4. The brief description of the test performed in this study are presented in the following sections.

Table 3-4: Standard Tests

Test	Standard	Specimen Dimensions	Number of Specimens Per Concrete Type
Concrete Slump (Workability)	ASTM C 143	N/A	N/A
Fresh Density	ASTM C 138	N/A	N/A
Compressive Strength	ASTM C 39	100Ø x 200 mm (4Ø x 8")	9
Splitting Tensile Strength	ASTM C 496	150Ø x 300 mm (6Ø x 12")	1
Flexural Strength (MOR)	ASTM C 78	150x150x500 mm (6 x 6 x 20")	1
Average Residual Strength (ARS)	ASTM C 1399	50x50x300 mm (2 x 2 x 12")	3
Unrestrained Drying Shrinkage	ASTM C 490	50x50x250 mm (2 x 2 x 10")	3
Surface Resistivity	AASHTO TP-95	100Ø x 200 mm (4Ø x 8")	3

3.5.1 Fresh Properties Evaluation of Concrete Mixtures

3.5.1.1 Slump Test

The slump of all concrete mixtures were measured by the slump test. The freshly mixed concrete is placed and rodded in a cone to measure the slump. The test is performed as per ASTM C 143, "Standard Test Method for Slump of Hydraulic-Cement Concrete" [87]. The cone mold is placed on top of a flat surface, filled with freshly mixed concrete in three layers and rodded 25 times per layer uniformly over the cross section with the rounded end of the tamping rod. After the top layer is placed, rodded, and cleaned of any excess concrete the mold is raised and the concrete allowed to subside. The vertical distance between the original and displaced position at the center of the top of the concrete is measured and taken as the slump value of the concrete. A typical setup for the slump test is shown in Figure 3-5.

Figure 3-5: (Left) Slump Test Set-Up, (Right) Measuring Slump of Concrete Mix

3.5.1.2 Concrete Unit Weight Test

The unit weight of each concrete mix were measured by the unit weight test. The freshly mixed concrete is placed and rodded in a cylindrical container made of steel to measure the concrete unit weight. The test is performed as per ASTM C 138, "Standard Test Method for

Density (Unit Weight), Yield, and Air Content (Gravimetric) of Concrete" [88]. The cylindrical mold is placed on a flat surface, filled with freshly mixed concrete in three layer and rodded 25 times per layer, uniformly over the cross section with the tamping rod. After the final layer has been placed and rodded, the top layer is to be strike-off and finished to produce a smooth top layer surface. Once the top layer is smoothed, the sides of the cylinder must be cleaned and any excess material removed before taking the appropriate reading. A typical setup for the concrete unit weight test is shown in Figure 3-6.

Figure 3-6: (Left) Unit Weight Test Set-Up, (Right) Measuring Unit Weight of Concrete Mix

3.5.2 Mechanical Properties Evaluation of Concrete Mixtures

3.5.2.1 Compressive Strength Test

The compressive strength of all concrete mixtures was determined using a 100 x 200mm (4 x 8 in.) concrete cylinders at 7, 14, and 28 days. The average compressive strength of three cylinders was taken as the compressive strength of that mixture. The sample preparation and test was performed as per ASTM C39, "Standard Test Method for Compressive Strength of Cylindrical Concrete Specimens" [89]. All cylinders were moist cured in the curing room at room temperature and at 95% or higher humidity until the day of testing. Cylinders were

removed from the curing room and excess moisture on the surface was wiped off. Cylinders were then capped using neoprene caps and tested using a compression machine with 300,000 lbs (300 kip) capacity. During testing, the load was applied continuously and without shock at a loading rate of 0.15 to 0.35 MPa/s (20 to 50 psi/sec) until failure. The compressive strength was recorded from the compression machine reading. The compression machine utilized can be seen in Appendix-A and displayed the following values:

- Max load (lbf)
- Strength (psi)
- Average Load Rate (psi/sec or psi/min)

Figure 3-7 shows the compressive strength test set-up and a typical failure mode of a concrete cylinder.

Figure 3-7: Compressive Strength Test Set-Up, (Right) Typical Failure Mode of a Concrete Cylinder Under Compression

3.5.2.2 Tensile Strength Test

The splitting tensile strength of all concrete mixtures was determined using a 150 x 300mm (6 x 12 in.) concrete cylinder at 28 days. The sample preparation and testing were performed

as per ASTM C 496, “Standard Test Method for Splitting Tensile Strength of Cylindrical Concrete Specimens” [90]. For this test, concrete cylinders were all cured in the curing room at room temperature and 95% or higher humidity until the day of testing. Cylinders were removed from the curing room and excess moisture on the surface was wiped off. The cylinders were marked, measured and placed longitudinally on the loading machine similar to the compression test. A plywood strip at the top and bottom of the specimen was placed along the center of the lower bearing block of the loading machine and the specimen. Then, a supplementary bearing plate was placed on top of the plywood strip and centered on the line marked on the specimen and the thrust of the spherical block. The load was applied continuously and without shock at a loading rate of 0.7 to 1.4 MPa/min (100 to 200 psi/min) until failure. The tensile strength was recorded from the compression machine reading. Figure 3-8 shows the splitting tensile strength test set-up and a typical failure mode of a concrete cylinder.

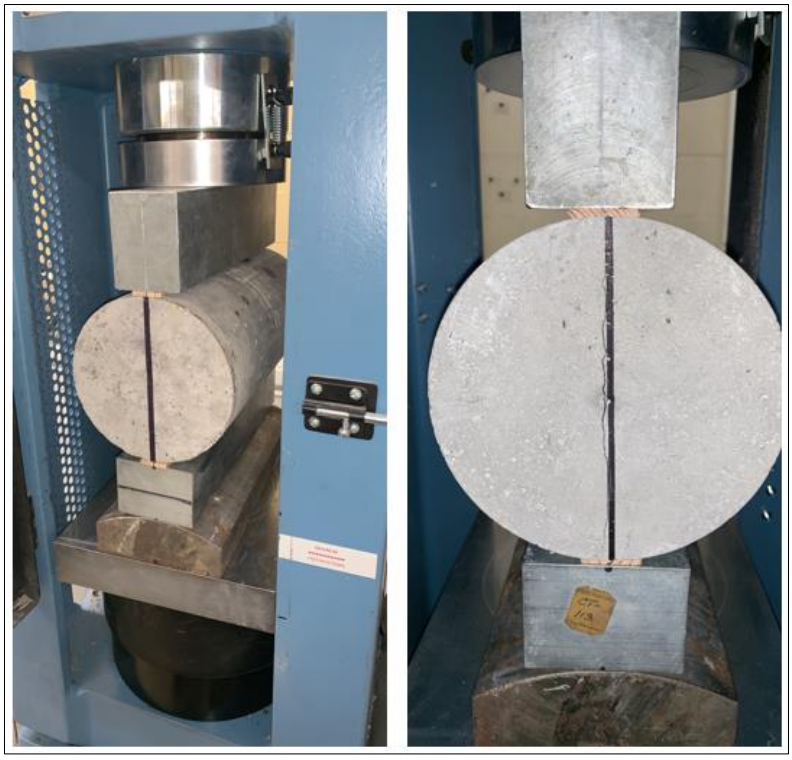

Figure 3-8: (Left) Splitting Tensile Strength Test Set-Up, (Right) Typical Failure Mode of a Concrete Cylinder Under Tension

3.5.2.3 Flexural Strength test

The flexural strength of all concrete mixtures was measured using a 150 x 150 x 500mm (6 x 6 x 20 in.) concrete beam at 28 days. The sample preparation and testing were performed as per ASTM C 78, “Standard Test Method for Flexural Strength of Concrete (Using Simple Beam with Third-Point Loading)” [91]. For this test, the concrete beam was cured in the curing room at room temperature and 95% or higher humidity until the day of testing. The beam was removed from the curing and excess moisture on the surface was wiped off. The beam was marked, measured and placed longitudinally on the support frame. The support frame along with the beam were placed on the loading machine and positioned in the center. The load applying blocks were then placed on the marked lines. The load was applied continuously and without shock at a loading rate of 0.86 to 1.21 MPa/min (125 to 175 psi/min) until failure. The flexural strength was recorded from the compression machine reading. Figure 3-9 shows the flexural strength test set-up and a typical failure mode of a concrete beam.

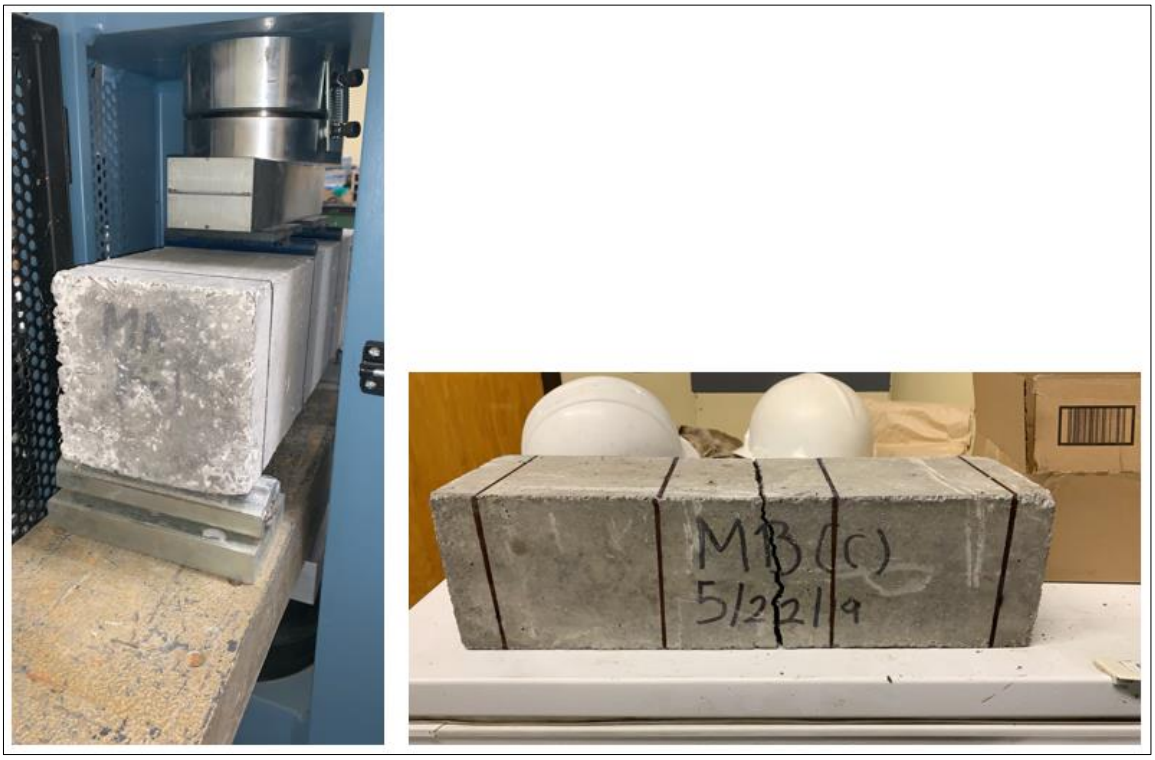

Figure 3-9: (Left) Flexural Strength Test Set-Up, (Right) Typical Failure Mode of a Concrete Cylinder Under Third-Point Loading

3.5.2.4 Average Residual Strength Test

The average residual strength of all concrete mixtures was determined using 50 x 50 x 300mm (2 x 2 x 12 in.) concrete beams at 28 days. The sample preparation and test was performed as per ASTM C 1399, "Standard Test Method for Obtaining Average Residual-Strength of Fiber-Reinforced Concrete" [92]. For this test, the concrete beams were cured in the curing room at room temperature and 95% or higher humidity until the day of testing. The beams were removed from the curing room and excess moisture on the surface was wiped off. The beams were marked, measured and placed on top of a stainless-steel plate for the first part of the test, longitudinally on the support frame. The support frame, steel plate and the beam were placed on the loading machine and positioned on the center plate. The loading head was then placed on the marked lines. An LVDT (Linear Variable Differential Transformer) was placed at the side of the specimen to measure deflection. The load cell and LVDT were connected to a data acquisition system that displayed the load applied (kN) and net deflection (mm) of the test beam at mid-span. The load rate was applied continuously and without shock at a loading movement rate of 0.65 ± 0.15 mm/min (0.025 ± 0.005 in/min) until a net deflection of 0.20mm (0.008 in.) was reached. The test is stopped and data is recorded as the initial loading (load-deflection) curve. The test is resumed by removing the steel plate, zeroing data acquisition devices and reloading the cracked beam at a loading rate of 0.65 ± 0.15 mm/min (0.025 ± 0.005 in/min) until a net deflection of 1.25mm (0.050 in.) is obtained. The average residual strength (ARS) for each beam is calculated using the following equation:

$$ARS = ((P_A + P_B + P_C + P_D)/4) \times k \quad (2)$$

Where:

k= L/bd^2, mm^{-2} (in^{-2})

ARS= Average residual strength, MPa (psi)

P_A= Recorded load at deflection of 0.50 mm (0.020 in.), N (lbf)

P_B= Recorded load at deflection of 0.75 mm (0.030 in.), N (lbf)

P_C= Recorded load at deflection of 1.00 mm (0.040 in.), N (lbf)

P_D= Recorded load at deflection of 1.25 mm (0.050 in.), N (lbf)

L= Span length, mm (in.)

b= Average width of beam, mm (in.)

d= Average depth of beam, mm (in.)

Figure 3-10 shows the average residual strength test set-up and a typical failure mode of a concrete beam.

Figure 3-10: (Left) ARS Initial Loading Test Set-Up, (Top Right) ARS Reloading Test Set-up (Bottom Right) Typical Failure Mode of ARS Beam Under Third-Point Loading

3.5.3 Durability Properties Evaluation of Concrete Mixture

3.5.3.1 Surface Resistivity Test

The surface resistivity of all concrete mixtures was determined using a 100 x 200mm (4 x 8 in.) concrete cylinders at 28 days with a 4-pin Wenner Probe, shown in Figure 3-11. The sample preparation was conducted as per ASTM C39, "Standard Test Method for Compressive Strength of Cylindrical Concrete Specimens" [89] and test was done as per AASHTO T 358, "Standard Method of Test for Surface Resistivity Indication of Concrete's

Ability to Resist Chloride Ion Penetration" [93]. For this test, the concrete cylinder was cured in the curing room at room temperature and 95% or higher humidity until the day of testing. The cylinders were removed from the curing and marked with four circumferential marks at 0, 90, 180, and 270 degrees, counterclockwise. The cylinders were also marked longitudinally at the center to use as a visual reference during testing. Once the beams were marked they were placed back in the curing room until the time of testing. The cylinders were then removed and transported to the specimen holder and cleaned with a saturated towel to maintain a saturated wet surface during testing. The 4-pin Wenner Probe was then used to take measurements along the longitudinal side of the sample while making sure the longitudinal center mark was equidistant between the two inner probe pins. Readings were taken at each circumferential mark by rotating the specimen counterclockwise. A total of eight readings (two per mark) were taken and an average was taken for each mark. Three cylinder specimens were used for each test and the average of all three is taken as the surface resistivity value for each mix. Figure 3-11 shows the surface resistivity 4-pin Wenner Probe used and a typical test being performed.

Figure 3-11: (Left) 4-Pin Wenner Probe, (Right) Surface Resistivity Test Set-Up

3.5.3.2 Unrestrained Drying Shrinkage Test

The unrestrained (free) shrinkage for all concrete mixtures was measured using the digital comparator test set-up as shown in Figure 3-12. The test consists of a sturdy upright support with a digital indicator gauge mounted on the top and a reference bar. The digital indicator has a range of 12.7mm (0.5 in.) and 0.00127mm (0.00005 in.) divisions. The unrestrained shrinkage of all concrete mixtures was measured using 50 x 50 x 250mm (2 x 2 x 10 in.) concrete prisms. From each concrete mixture, three concrete prisms were prepared as previously described. Both mold prisms used were covered with wet towels and left undisturbed for 24 hours. They were then unmolded and placed in the curing room at room temperature and 95% or higher humidity for 15 minutes and the initial 24-hour reading was taken. Then they were continuously moist cured for 7 days followed by air curing at normal room temperature.

The change in length for prisms was measured in accordance with ASTM C 490, “Standard Practice for Use of Apparatus for The Determination of Length Change of Hardened Cement Paste, Mortar, and Concrete” [86]. The change in length for each prism was recorded after 7 days of casting and once a week thereafter for 91 days. Figure 3-12 shows the Comparator test set-up and a concrete specimen being tested.

Figure 3-12: (Left) Unrestrained Drying Strength Test Set-Up, (Right) Unrestrained Drying Shrinkage Test Reading

CHAPTER 4: EXPERIMENTAL RESULTS AND DISCUSSION

4.1 INTRODUCTION

This chapter discusses the outcomes of the experimental program described in Chapter 3. The major aim of this research is to investigate the effects of basalt fiber in BFRC. For that, a total of 14 concrete mixtures were designed and divided into two groups; the first group consists of a control mix, 15% BF, 30% BF, 45% BF and 50% BF mix (by volume) as well as 30% SF and 50% SF mix utilizing a w/c of 0.35. The second group consists the same mix volumes, utilizing a w/c of 0.40. The fresh properties examined are the slump and concrete unit weight, as presented in Table 4-1. The mechanical properties tested are the compressive strength at 7, 14, and 28 days, the tensile strength at 28 days, flexural strength at 28 days, and the average residual strength at 28 days, presented in Table 4-2. The durability properties examined are the unrestrained drying shrinkage up to 91 days, surface resistivity at 28 days, and corrosion rates and corrosion potential. Refer to Chapter 3 for explanation of the tests mentioned and refer to Chapter 5 for explanation of corrosion rates and corrosion potential tests.

4.2 FRESH PROPERTIES OF FRC MIXTURES

The fresh properties of the concrete mixtures investigated are slump and unit weight. Slump of a concrete mixture is used as a monitor technique for the consistency and workability of unhardened concrete. With the addition of fibers, slump values are known to decrease and thus HRWA are added to the mix in order to achieve the desirable slump value. Slump values are also generally found to increase proportionally with the w/c ratio and thus is said to be inversely related to the concrete strength. Theoretical values for the amounts of HRWA were used by [17, 78, 79, 80] as a guide to achieve desired slump values.

The fresh properties of the concrete mixtures were also investigated by the unit weight test. The unit weight of the mix is used as a monitor technique for volume of mix, and air content values. Unit weight is affected by the air content within the mix, which also affects the slump of the mix. When slump decreases, the air content generally increases which should reduce the unit weight value. The density of a concrete mixture is said to influence the compressive and durability properties of the hardened concrete. A denser concrete generally provides higher strength concrete due to the fewer amount of voids and porosity within the mix, which

also provides a less permeable mix thus improving durability. Table 4-1 shows the slump values for all mixtures measured in this study, amount of HRWA used to achieve a desired slump of 6 in. ± 2 in. and the unit weight values of all mixtures.

Table 4-1: Fresh Properties of Concrete Mixtures

Fresh Properties				
Group (W/C Ratio)	**Mixture**	**Slump (inch)**	**HRWA (ml)**	**Unit Weight (Kg/cm^3)**
Group I (0.35)	MA (Control)	5.0	0.00	2286.379
	MA (15)	5.5	28.89	2286.896
	MA (30)	6.5	57.78	2423.624
	MA (45)	5.5	86.67	2415.094
	MA (50)	5.5	30.00	2366.503
	MA (Steel 30)	6.0	50.0	2443.267
	MA (Steel 50)	6.0	40.0	2468.338
Group II (0.40)	MB (Control)	4.5	0.00	2411.217
	MB (15)	6.5	28.89	2393.125
	MB (30)	6.5	57.78	2455.415
	MB (45)	5.5	75.25	2402.688
	MB (50)	5.5	30.0	2398.553
	MB (Steel 30)	6.0	35.0	2434.996
	MB (Steel 50)	6.0	25.0	2442.492

As can be seen from Table 4-1, the slump values were kept within the target range of 6 in. ± 2 in. The HRWA values reached a maximum of 86.67ml for mixture (MA 45), which provided a slump of 5.5 in. The control mixtures did not require any HRWA as no fibers were used for these mixtures. The steel fiber mixtures required less HRWA when compared to the basalt fiber mixtures with the same fiber per volume mixtures. This can be attributed to the surface area covered by the steel fibers, being less than that of the basalt fibers which would provide a lower slump and as such required less HRWA to achieve the target slump range. This is also

attributed to the material, especially the density of the fibers being used. HRWA amounts required are as expected; increasing as the volume fibers increased and requiring less for the higher w/c mixtures (MB). Except for the two mixtures (MA (50) and MB (50)) this could be attributed to an error during mixing or while performing the slump test. Overall the results indicate that as fiber volume increases and as w/c ratio increases, slump decreases and thus HRWA amounts required increases.

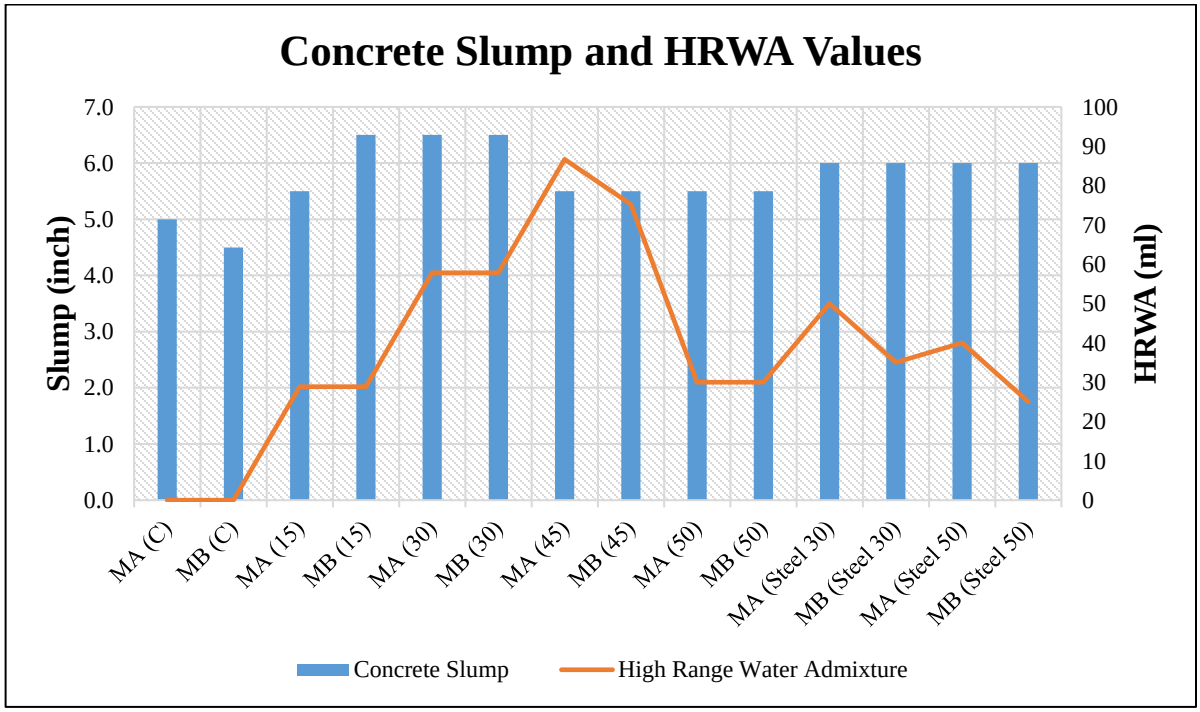

Figure 4-1: Concrete Slump and HRWA Graph

The concrete unit weight values can be seen in Table 4-1. The results correlate closely with the slump values obtained from the slump test, where a higher fiber volume obtained, a higher concrete unit weight with MB (30) obtaining the highest unit weight of 2455.415 kg/m^3 (153.28 lb./ft^3) for BFRC mix and a unit weight of 2468.338 kg/m^3 (154.10 lb./ft^3) for SFRC (MA (Steel 50)). The results are as expected, higher fiber volumes increase the unit weight of the concrete until a certain volume, in this case 0.30% for BF. After which, the unit weight decreases due to the increased voids created by the fibers within the concrete matrix. Steel fibers displayed the highest unit weight results, due to the density of the fibers, as expected.

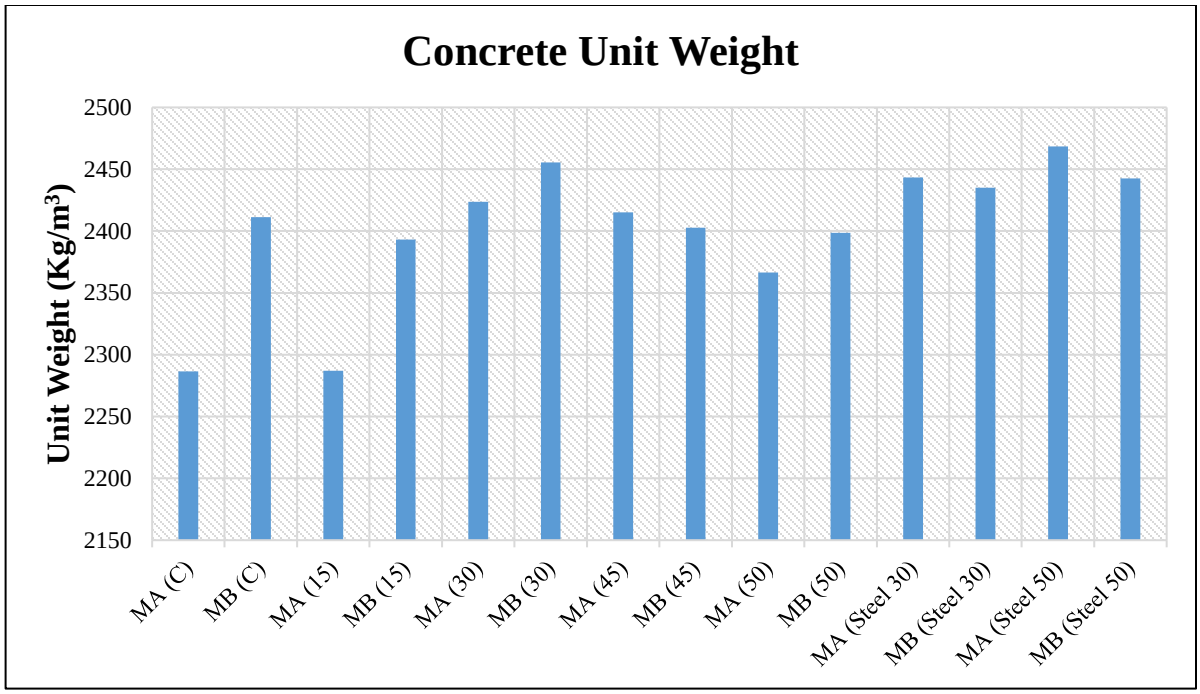

Figure 4-2: Concrete Unit Weight Graph

4.2.1 The Effect of Fibers on Fresh Properties of FRC

The effect of basalt and steel fibers on the fresh properties of the FRC mixtures observed from the above data are listed below.

1) As expected, the addition of fibers increased the slump of the concrete which required an increase in the HRWA amount. The increase of HRWA was up to 86.67 ml when 0.45% BF was used for MA and up to 75.25 ml when 0.45% BF was used for MB to provide a slump of 5.5 in. for both mixes.
2) The increase of HRWA for SF was up to 50.00 ml when 0.30% SF was used for MA and up to 35.00 ml when 0.30% SF was used for MB to provide a slump of 6.0 in. for both mixes.
3) The increase in w/c ratio, from 0.35 to 0.40 (MA, MB), displayed no significant effect in the amount of HRWA required to reach desired slump values for BF. The effects are noticeable for SF, where MB required less HRWA to provide the same slump values.
4) As expected, the addition of fibers increased the unit weight of the concrete. The increase in unit weight was up to 6.00% when a fiber volume of 0.30% BF was

introduced for MA and up to an increase of 1.83% when a fiber volume of 0.30% BF was introduced for MB.

5) The unit weight also increased with the addition of steel fibers. The increase in unit weight was up to 7.96% when 0.50% SF was introduced for MA and up to an increase of 1.30% when a fiber volume of 0.30% was introduced for MB.
6) The increase in w/c ratio, from 0.35 to 0.40 (MA, MB), displays mixed results for BF. An increase in unit weight is gained from increasing the w/c ratio up to a fiber volume of 0.30%. After which, unit weight values decrease.
7) The increase in w/c ratio, from 0.35 to 0.40 (MA, MB), displayed a decrease in unit weight for SF.

4.3 MECHANICAL PROPERTIES OF FRC MIXTURES

The compressive strength, tensile strength, flexural strength and average residual strengths are considered the most important mechanical properties of FRC and they were investigated for all concrete mixtures considered. The compressive strength was measured at different ages (7, 14, and 28 days) to determine the early age effect of fibers on the mechanical properties as well as standard 28 day curing period. The tensile and flexural strength, however, was only measured at 28-days to determine the effects an increased fiber volume on the mechanical properties of the concrete mix. Average residual strength (ARS) was also measured at 28-days, this test is exclusive to FRC mixtures and provides an insight into the improved mechanical toughness of concrete with the addition of fibers. Results of the compressive, tensile, flexural and average residual strengths are shown in Table 4-2.

Table 4-2: Mechanical Properties of Concrete Mixtures

Mechanical Properties							
Group (W/C Ratio)	**Mixture**	**f'_c (psi) 7 days**	**f'_c (psi) 14 days**	**f'_c (psi) 28 days**	**f_t (psi) 28 days**	**MR (psi) 28 days**	**ARS (psi) 28 days**
Group I (0.35)	MA (Control)	5712.5	8479.4	9894.7	493.5	580.8	N/A
	MA (15)	5942.9	6723.8	7209.8	582.9	611.7	42.1
	MA (30)	6219.2	6982.2	7900.1	593.6	723.3	82.7
	MA (45)	5849.4	6840.1	7412.3	613.2	680.0	110.2
	MA (50)	6229.6	6505.9	7556.3	636.2	650.8	149.4
	MA (Steel 30)	5710.0	6561.4	7413.4	527.5	705.0	130.5
	MA (Steel 50)	6214.5	7015.0	7803.5	611.8	685.0	165.3
Group II (0.40)	MB (Control)	5622.7	6209.9	6854.5	467.9	467.9	N/A
	MB (15)	4758.6	5484.9	6573.5	489.2	558.4	14.5
	MB (30)	5268.6	5764.4	6921.7	554.1	657.5	50.8
	MB (45)	4203.6	5599.9	6246.0	482.3	682.5	62.4
	MB (50)	4764.6	5454.7	6401.0	577.6	658.3	95.7
	MB (Steel 30)	4656.9	5641.0	6369.9	485.6	632.5	88.5
	MB (Steel 50)	4901.7	5783.2	6201.7	485.2	610.0	153.7

4.3.1 The Effect of Fibers on The Compressive Strength of FRC

The compressive strength of concrete is the most common performance attribute used when designing structures. Compressive strengths tests are utilized as a basis for quality control of concrete proportioning, mixing, and placing operations. Concrete cylinders are typically cast and cured for 28 days to attain the 28-day compressive strength of the concrete, which is used to evaluate the design strength of the mixture.

The addition of fibers in concrete has shown mixed results concerning compressive strength at 28-days. From literature, it was assumed that the additions of fibers would reduce the 28-day compressive strength when utilizing fiber volumes less than 2% per volume. This may be attributed to the increased voids and reduced bond area between aggregates and cement

matrix. Increasing the fiber volumes past 2% is not a feasible solution if higher compressive strength is to be achieved. The usage of fibers at low dosages (<1% per volume) is not intended to increase the compressive strength of the concrete. On the other hand, reducing the w/c ratio is known to decrease the strength of the concrete and so Group II (MB) should experience a decrease in compressive strength. The results for the compressive strength of the mixtures can be seen in Table 4-2 as well as shown in Figure 4-3.

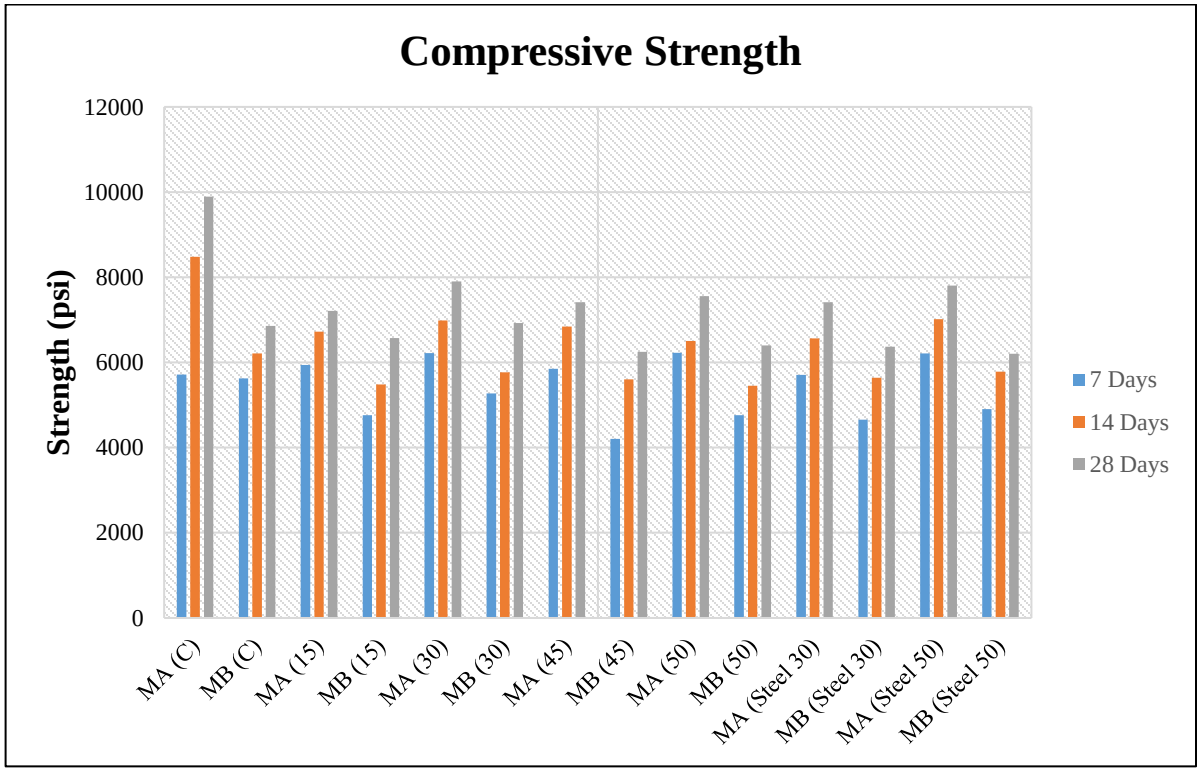

Figure 4-3: Concrete Compressive Strength Graph

As can be seen from Figure 4-3, the addition of fibers shows an overall decrease in compressive strength at 28 days for both MA and MB samples. The early age (7-days) compressive strength, on the other hand, tends to increase with the addition of fibers for MA, but tends to decrease for MB due to the higher w/c ratio used in the second group of mixtures. As expected, MA compressive values are significantly higher than MB and the use of steel fibers showed similar strengths when compared to the same basalt fiber volume utilized for both mix groups. Overall, all mixtures showed a higher compressive strength compared to the target design strength (5075 psi).

The effects of the addition of fibers on the compressive strength of FRC were investigated and are listed below:

1) The addition of fibers decreased overall compressive strengths at 28-days.
2) Group I (MA) showed an overall increase in early age strength (7-day) up to an increase of 9.05% for MA (50).
3) The addition of fibers decreased overall compressive strengths for mix Group II (MB), with the exception of MB (30) with an increase in 28-day strength of 0.98%
4) As expected, an increase in w/c ratio decreased the compressive strength of all concrete mixtures.
5) The use of steel fibers had little effect on the compressive strength values when compared to the same basalt fiber volumes used for both mix groups.
6) The highest early-age strength (7-day) experienced by steel fibers is by Group I MA (Steel 50) with an increase of 8.79%.

4.3.2 The Effect of Fibers on The Splitting Tensile Strength of FRC

The tensile strength of concrete is another important property that is used in the design of structural concrete members and to determine the development length of reinforcement. Concrete cylinders are typically casted and cured for 28 days to attain the 28-day splitting tensile strength of the concrete.

The addition of fibers in concrete has shown to improve the tensile strength of concrete, as the fiber volumes tend to increase, the ductility of the material is improved and provides resistance against longitudinal crack growths. From literature, it was assumed that the additions of fibers would increase the 28-day tensile strength with an increase in fiber volume. The main reason to this may be attributed to the bridging interaction created by the fibers in preventing further crack growths. This interaction allows the concrete to withstand higher loads that would otherwise create macrocracks that would cause the material to fail. The usage of fibers at low dosages (<1% per volume) is mainly implemented to prevent macro cracks and so an increase in tensile strength was predicted. The reduction of the w/c ratio is known to decrease the strength of the concrete and so Group II (MB) should see a decrease in tensile strength. The results for the tensile strength of the mixtures can be seen in Table 4-2 as well as in Figure 4-4.

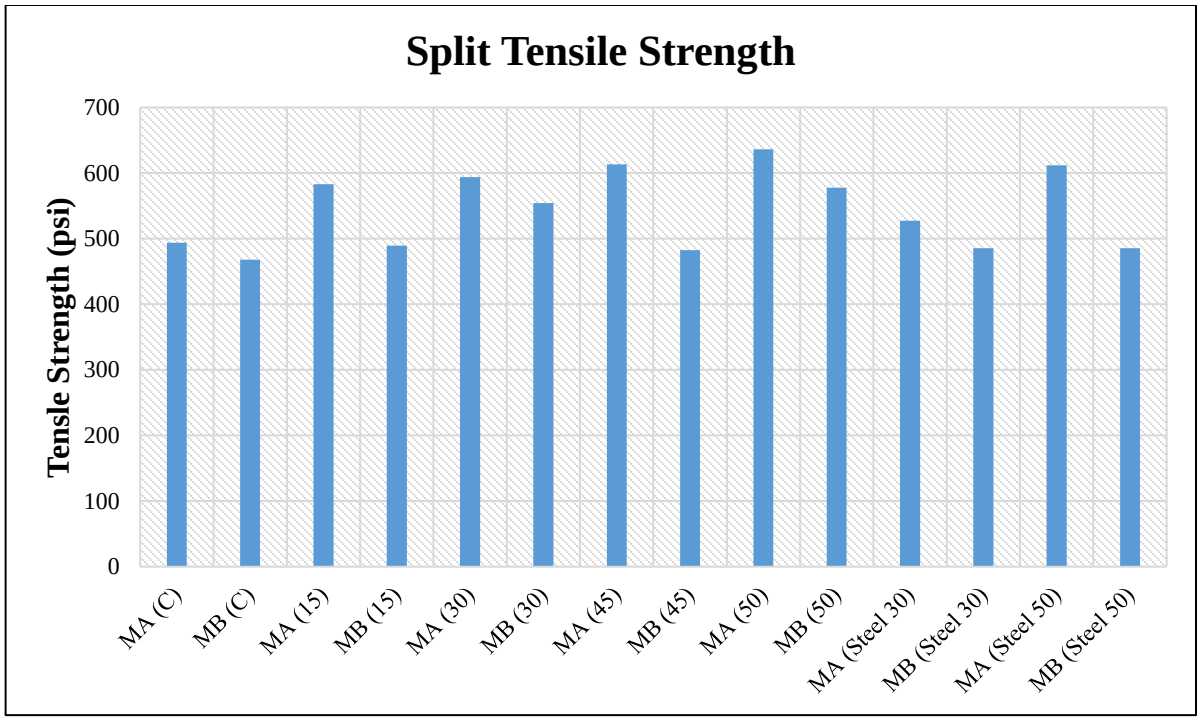

Figure 4-4: Concrete Split Tensile Strength Graph

As can be seen from Figure 4-4, the addition of fibers shows an increase in tensile strength in relation to fiber volume for both MA and MB samples. The highest tensile strength experienced by Group I is by MA (50) with an increase of 28.92% and for Group II is by MB (50) with an increase of 23.45%. As expected, MA tensile strength values are higher than MB due to the w/c ratio difference. On the other hand, the use of steel fibers showed a lower tensile strength when compared to the same basalt fiber volume utilized for both mix groups. In general, the tensile strength data demonstrate the beneficial effect of implementing fibers. This may be attributed to the fibers bridging micro and macro-cracks within the matrix, delaying the formation of the splitting crack.

The effects of the addition of fibers on the tensile strength of FRC were investigated and are listed below:

1) The addition of fibers increased overall tensile strength at 28-days for both Group I (MA) and Group II (MB).
2) The highest tensile strength experienced in Group I is by MA (50) with an increase of 28.92% and for Group II is by MB (50) with an increase of 23.45%.

3) As expected, an increase in w/c ratio decreased the tensile strength of the concrete mixtures.
4) The use of steel fibers showed a lesser effect, when compared to the same basalt fiber volume, in increasing tensile strength.
5) Group I MA (Steel 50) showed an increase of 23.97% and Group II MA (Steel 50) showed an increase of 3.70%.

4.3.3 The Effect of Fibers on The Flexural Strength of FRC

The flexural strength of concrete is one measure of the tensile strength of concrete and is used to measure the ability of concrete to resist failure under bending. Concrete prism specimens are typically casted and cured for 28 days to attain the 28-day flexural strength of the concrete, also known as the modulus of rupture (MR), which may be used to evaluate the design strength of the mixture. The flexural MR is about 10 to 20% of the compressive strength depending on the type, size and volume of coarse aggregates used. The type of loading may differ MR values, where third-point loading may provide higher MR values compared to center-point loading, up to about 15% higher.

The addition of fibers has shown to improve the flexural strength of concrete, as the fibers increase the ductility of the material. This increase in ductility offers resistance against micro and macro-cracks from propagating allowing the concrete to continue to sustain considerable loads, which provide higher flexural values. From literature, it was assumed that the addition of fibers would increase the 28-day flexural strength with an increase in fiber volume and should be correlated to the compressive strengths recorded. The main reason to this, may be attributed to the bridging interaction created by the fibers in preventing further crack growth. This interaction allows the concrete to withstand higher loads that would otherwise create macrocracks that would cause the material to fail. Although higher flexural values are expected, the usage of fibers is not to be used as a substitute for conventional reinforcement, especially at low dosages (<1% per volume). The results for the flexural strength (MR) of the mixtures can be seen in Table 4-2 as well as in Figure 4-5.

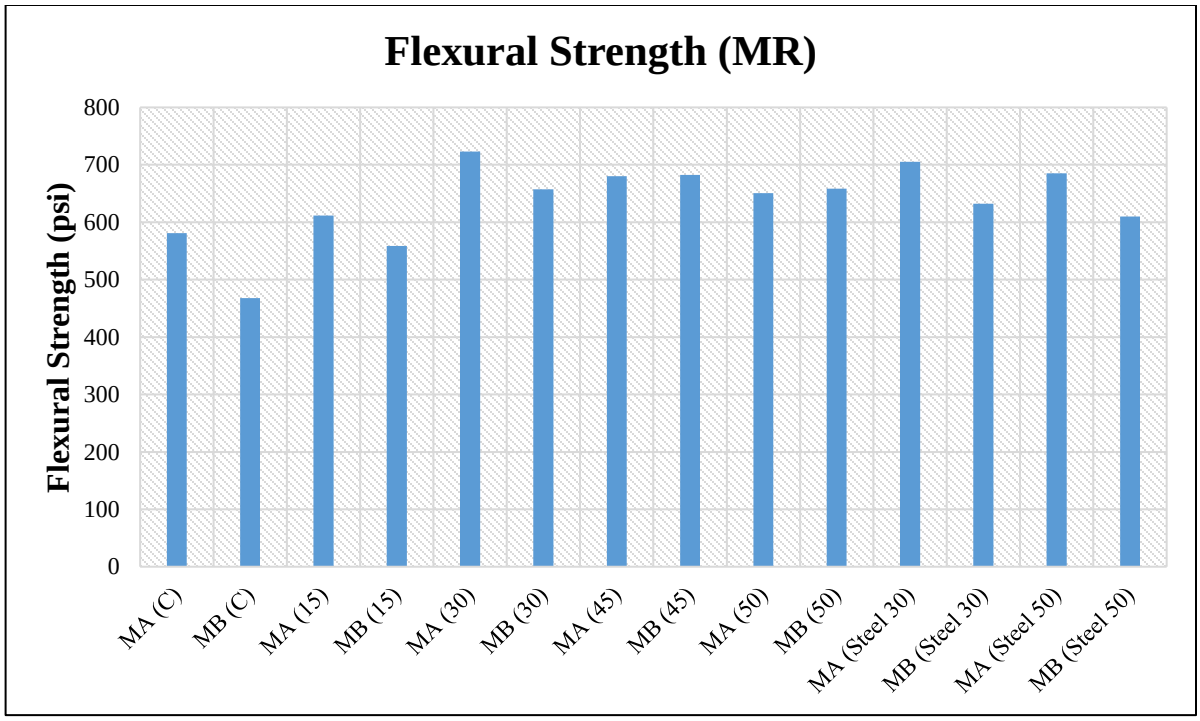

Figure 4-5: Concrete Flexural Strength Graph

As can be seen from Figure 4-5, the addition of fibers shows an increase in flexural strength in relation to fiber volume, up to a fiber volume of 0.30% for MA and up to a fiber volume of 0.45% for MB samples. The reason as to why 0.50% by volume did not provide higher values may be attributed to inefficiency of fibers at that volume. Although balling of fibers were not experienced, higher fiber volumes require more cementitious material to coat both the fiber and aggregates. This in return may explain the reduction in strength of the materials and would indicate that at lower fiber volumes (<1%), a fiber volume of around 0.30-0.45% would optimize the efficiency of the fibers.

The highest flexural strength experienced by Group I is by MA (30) with an increase of 24.54% and for Group II is by MB (45) with an increase of 45.86%. As expected, MA flexural strength values are significantly higher than MB and have a similar trend when compared to compressive strengths. On the other hand, the use of steel fibers showed a lower improvement to the flexural strength when compared to the same basalt fiber volume utilized for both mix groups. The highest flexural strength experienced by steel fibers in Group I is by MA (Steel 30) with an increase of 21.38% and for Group II is by MB (Steel 30) with an increase of 35.18%.

The effects of the addition of fibers on the flexural strength (MR) of FRC were investigated and are listed below:

1) The addition of fibers increased overall flexural strength at 28-days for both Group I (MA) and Group II (MB).
2) The highest flexural strength experienced in Group I is by MA (30) with an increase of 24.54% and for Group II is by MB (45) with an increase of 45.86%.
3) As expected, an increase in w/c ratio decreased the tensile strength of the concrete mixtures, which correlated to the compressive strength trend.
4) The use of steel fibers showed a lesser effect, when compared to the same basalt fiber volume, in increasing flexural strength.
5) The highest flexural strength by steel fibers is by Group I MA (Steel 30) which showed an increase of 21.38% and Group II MB (Steel 30) showed an increase of 35.18%.

4.3.4 The Effect of Fibers on The Average Residual Strength of FRC

The average residual strength is a measure of the post-cracking tensile strength of concrete. Concrete prism specimens are typically casted and cured for 28 days to attain the 28-day average residual strength (ARS) of the concrete, which may be used to evaluate the performance of fiber-reinforced concrete and to optimize the FRC mix proportions. The ARS values are mainly used to compare results among different fiber types including materials, dimension and shape and also different fiber contents.

The addition of fibers has shown to improve the residual strength of concrete, as the fibers increase the ductility of the material and act as a bridging mechanism preventing further crack growth. This improved ductility improves the capacity of the concrete to absorb energy during fracture which allows the concrete to sustain higher loads post-cracking where normal concrete would fail. This ability to absorb energy during fracture is referred to as toughness and is one of the most important benefits of the incorporation of fibers into plain concrete. From literature, it was assumed that the addition of fibers would increase the 28-day average residual strength with an increase in fiber volume. The main reason to this may be attributed to the bridging interaction created by the fibers in preventing further crack growth allowing the concrete to sustain loads post-cracking. Also, increased fiber volumes would theoretically provide more fibers per area of crack which should see an increase in ARS values. As for fiber

types, the mixtures with steel fibers should see higher ARS values since steel fibers have higher tensile strength compared to basalt fibers. The results for the average residual strength (ARS) of the mixtures can be seen in Table 4-2 as well as in Figure 4-6.

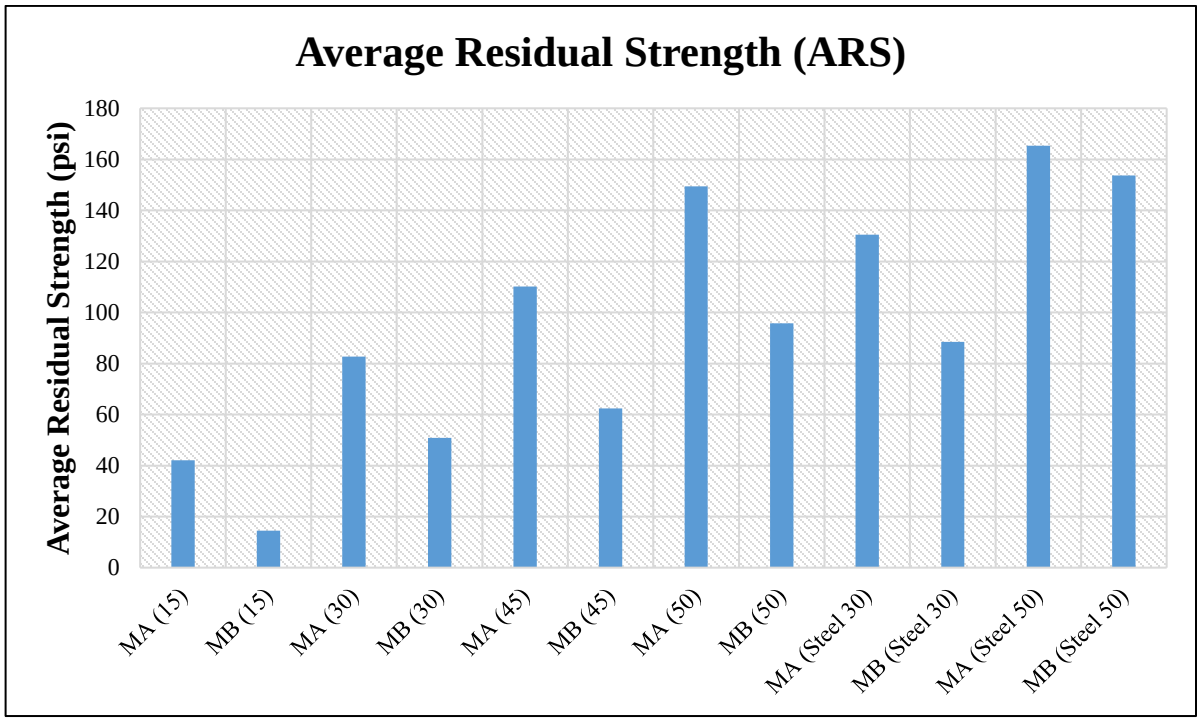

Figure 4-6: Average Residual Strength Graph

As can be seen from Figure 4-6, the addition of fibers increases the ARS of all mixtures with the increase in fiber volume. As expected, a fiber volume of 0.50% by volume, provided the highest ARS for basalt fibers and overall SFRC mixtures provided the highest results. The control samples displayed no residual strength due to the samples not being able to be reloaded for the second part of the test. As can be seen in Figures 4-7 and Figures 4-9, the load required to start crack propagation increases with respect to fiber volume. Once the first crack was observed, the test was stopped and the reloading part of the test was conducted. As can be seen in Figures 4-8 and Figures 4-10, the increase in fiber volume provides an improved toughness in the mixtures, which results in higher ARS values.

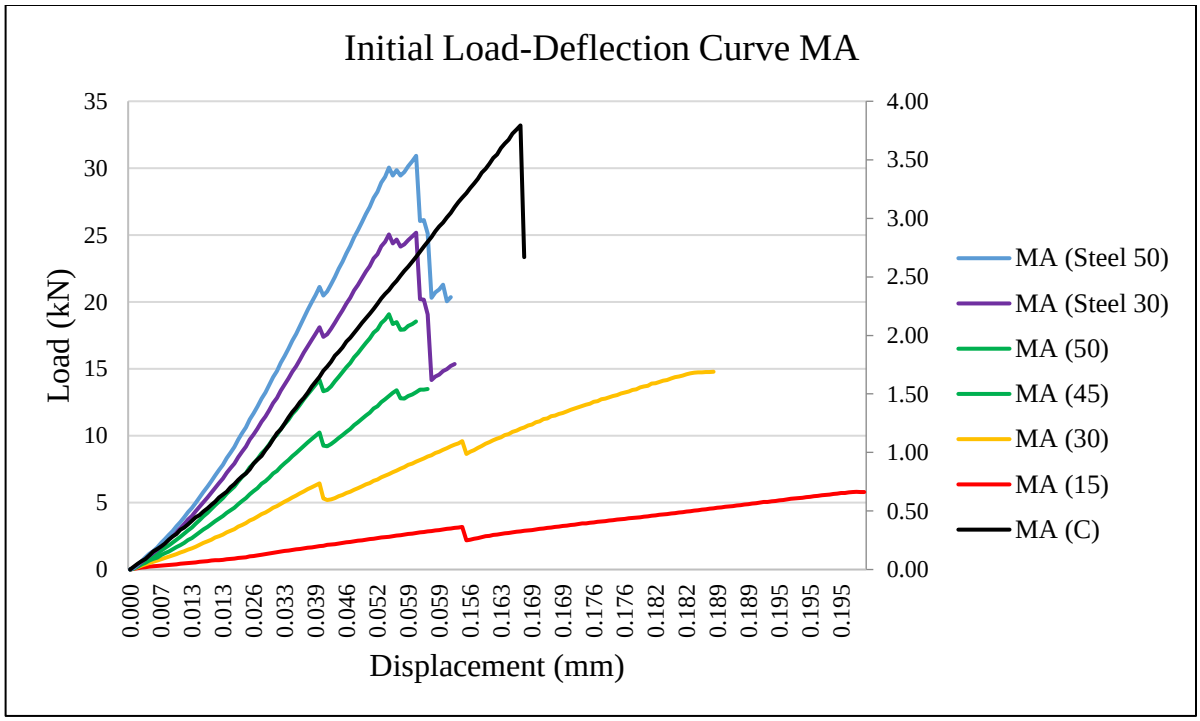

Figure 4-7: MA Initial Load-Deflection Curve Graph

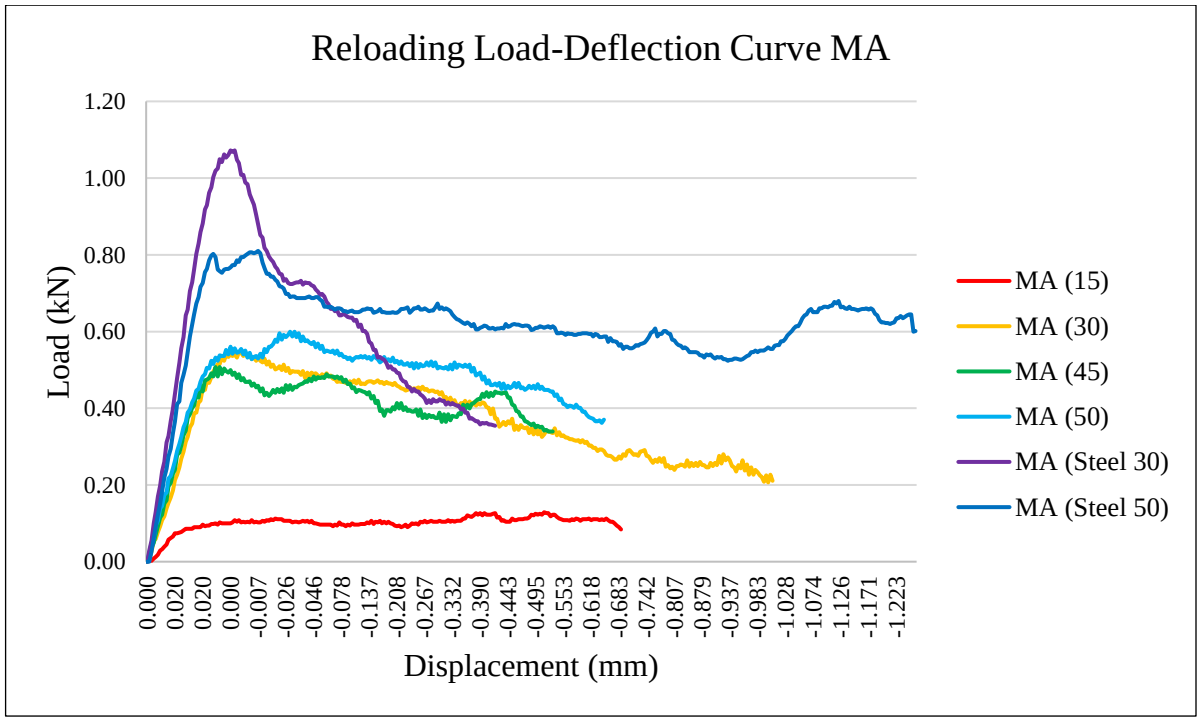

Figure 4-8: MA Reloading Load-Deflection Curve Graph

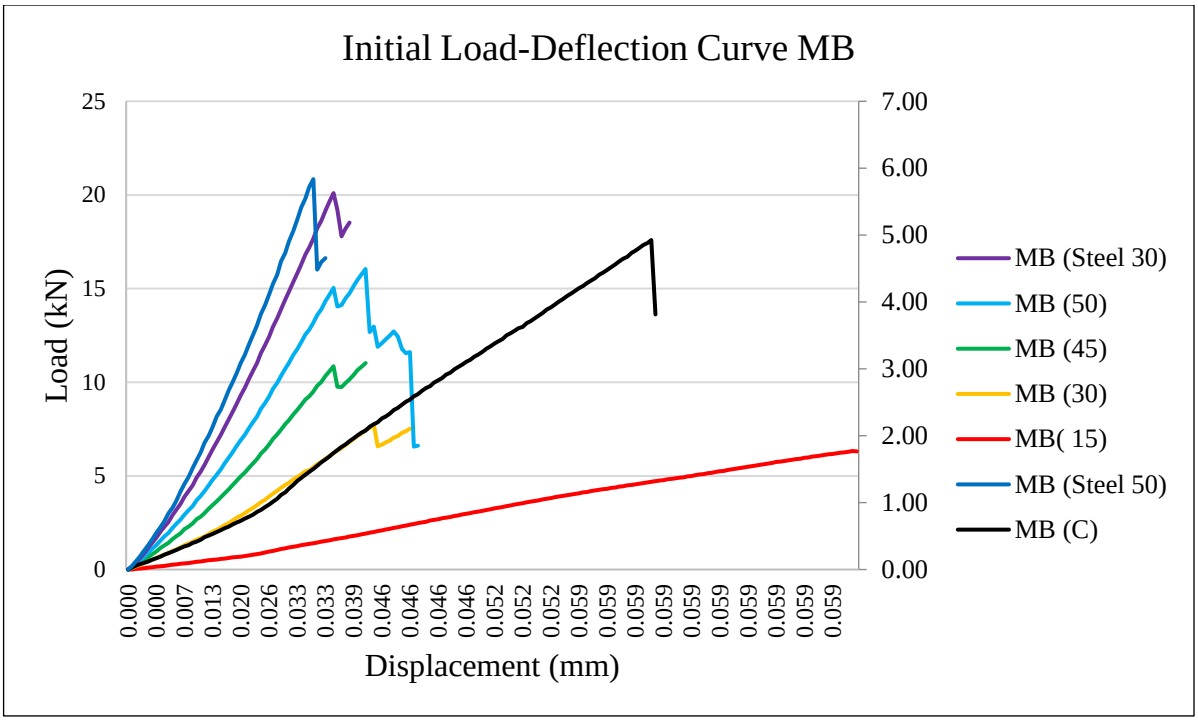

Figure 4-9: MB Initial Load-Displacement Curve Graph

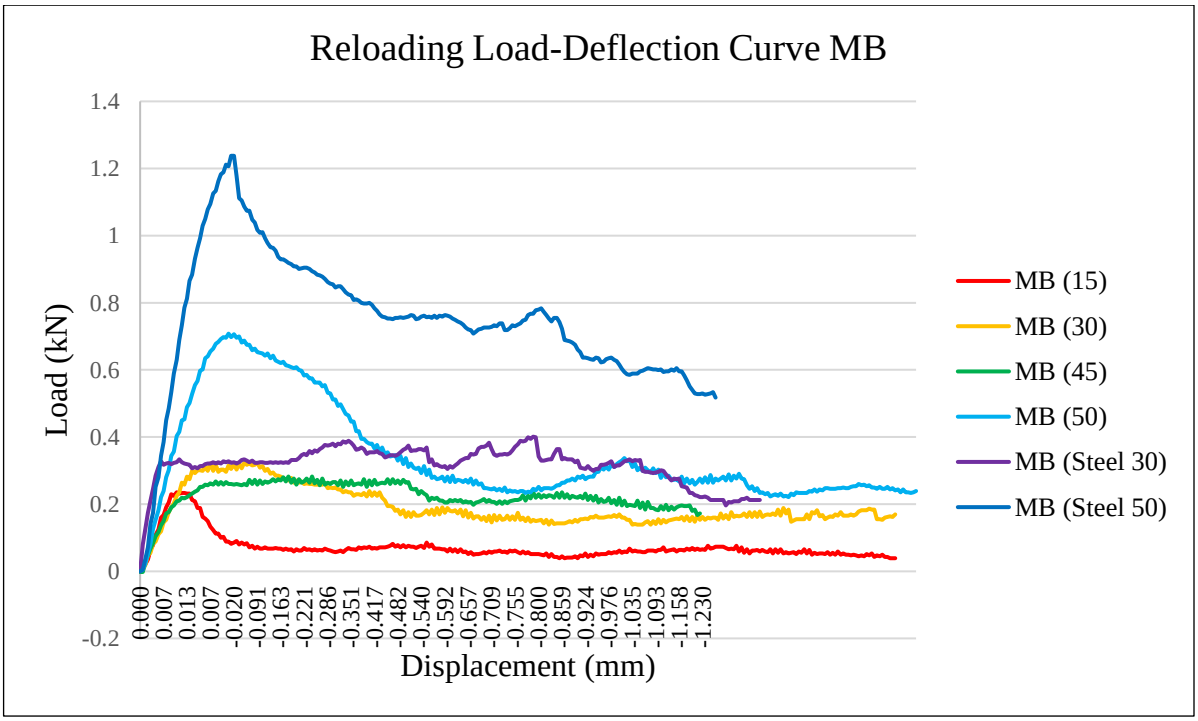

Figure 4-10: MB Reloading Load-Displacement Curve Graph

The test displays SFRC to be more effective in improving ARS. This may be attributed to the material properties of steel fibers being able to withstand more loads (higher modulus of

elasticity) and may also be attributed to the surface area covered by the fibers. The highest BFRC ARS is experienced by Group I is by MA (50) with an ARS of 149.0 psi and for Group II is by MB (50) with an ARS of 95.7 psi and as expected MA ARS values are significantly higher than MB. On the other hand, the use of steel fibers showed an improved ARS when compared to the same basalt fiber volume utilized for both mix groups. The highest flexural strength experienced by steel fibers in Group I is by MA (Steel 50) with an ARS of 165.3 psi and for Group II is by MB (Steel 50) with an ARS of 153.7 psi.

The effects of the addition of fibers on the average residual strength (ARS) of FRC were investigated and are listed below:

1) The addition of fibers increased overall ARS at 28-days for both Group I (MA) and Group II (MB).
2) The highest BF ARS experienced in Group I is by MA (50) with an ARS of 149.4 psi and for Group II is by MB (50) with an ARS of 95.7 psi.
3) As expected, an increase in w/c ratio significantly decreased the ARS of the concrete mixtures.
4) The use of steel fibers showed an improved residual strength when compared to the same basalt fiber volume, up to an increase of 11 % for MA 0.50% by volume and an increase of 40% for MB 0.50% by volume.
5) The highest strength by steel fibers is by Group I MA (Steel 50) with an ARS of 165.3 psi and Group II MA (Steel 50) with an ARS of 153.7 psi.

4.4 DURABILITY PROPERTIES OF FRC MIXTURES

The durability properties of the concrete mixtures were investigated by the unrestrained shrinkage and surface resistivity tests. The unrestrained shrinkage of all concrete mixtures in this study was measured using the comparator test set-up explained in Chapter 3. The free shrinkage was measured using 50 x 50 x 250mm (2 x 2 x 10 in.) concrete prisms prepared from each mixture and cured in the curing room with 95% or higher relative humidity for 7 days followed by curing at room temperature in the open air. The surface resistivity tests were measured using 100 x 200mm (4 x 8 in.) concrete cylinders at 28 days with a 4-pin Wenner Probe, shown in Figure 3-11 and explained in Chapter 3. The results for the unrestrained

shrinkage and surface resistivity tests of the mixtures can be seen in Figure 4-11 and Figure 4-12, respectively.

4.4.1 The Effect of Fibers on The Unrestrained Shrinkage of FRC

It is known that during the hardening process of concrete, there is a reduction of concrete volume due to the effects of cement hydration and water loss. With the addition of fibers, shrinkage values should theoretically see a decrease with increased fiber volume as the fibers will restrain the cementitious matrix from contracting. The increase in w/c ratio should see a decrease in shrinkage strain values as the concrete will have more water to be used in the cement hydration process allowing the concrete to not shrink for a longer period of time. The usage of steel fibers should see the most improvement in preventing shrinkage, as literature has shown steel fibers to be effective in this characteristic. The results for the unrestrained shrinkage can be seen in Figure 4-11.

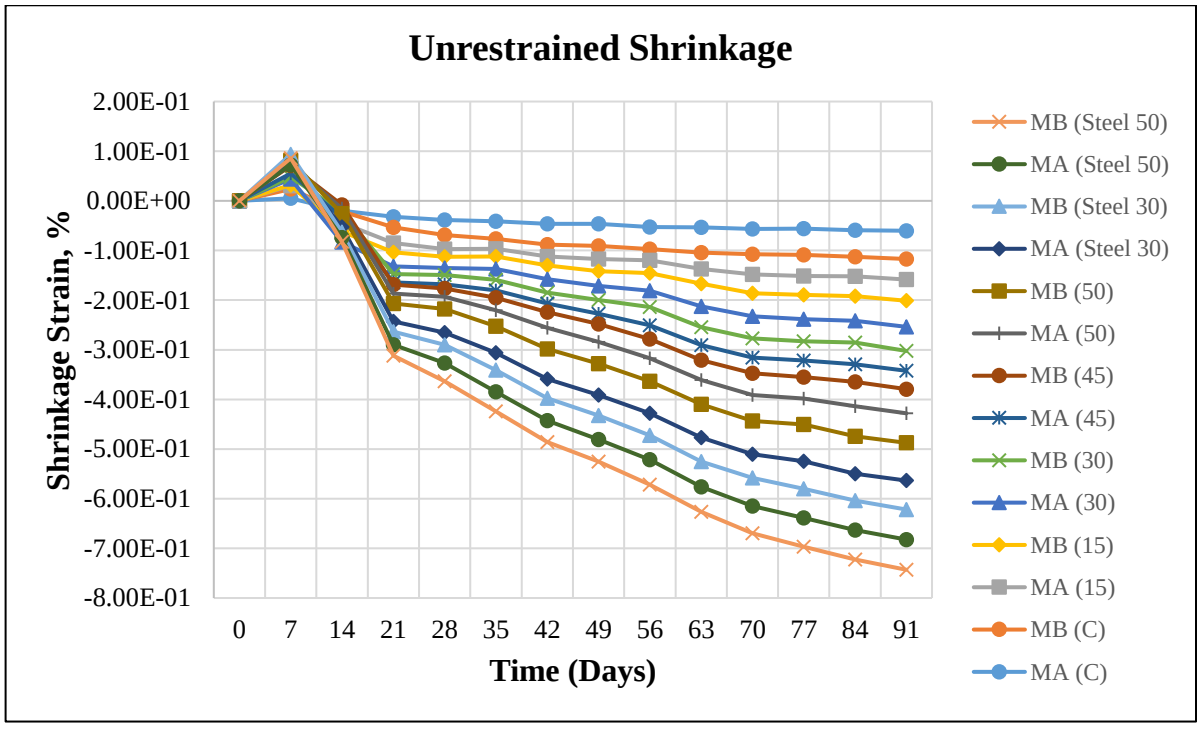

Figure 4-11: Unrestrained Shrinkage Graph

As can be seen from Figure 4-11, the addition of fibers shows reduced shrinkage strain in relation to the increase in fiber volumes. The graph shows expansion of all mixtures in the first 14 days which is attributed to the 7 day period of the samples being immersed in the

curing tank before being air dried. This allowed the samples to absorb water and increase their overall dimensions. All fiber samples followed a similar trend of decreased shrinkage strain values, whereas the control samples followed a more linear shrinkage trend. The use of steel fibers showed a significantly lower shrinkage strain when compared to the same basalt fiber volume utilized for both mix groups.

4.4.2 The Effect of Fibers on The Chloride Ion Penetrability of FRC

The surface resistivity test is a measure of the chloride ion penetrability of concrete. The test determines the electrical resistivity of water-saturated concrete to provide a rapid indication of its resistance to the penetration of chloride ions. This test method is used for the evaluation of materials and material proportions for design purposes as well as for research and development. Based on the literature, the inclusion of basalt fibers should show a decrease in chloride ion penetrability with increased fiber volume fractions. The increase in w/c ratio should increase the chloride ion penetrability as more voids and a higher porosity is attained by increasing w/c ratio. The inclusion of steel fibers should also see an increase in chloride ion penetrability due to the material characteristics of steel fibers. The results for the chloride ion penetrability of the concrete can be seen in Figure 4-12.

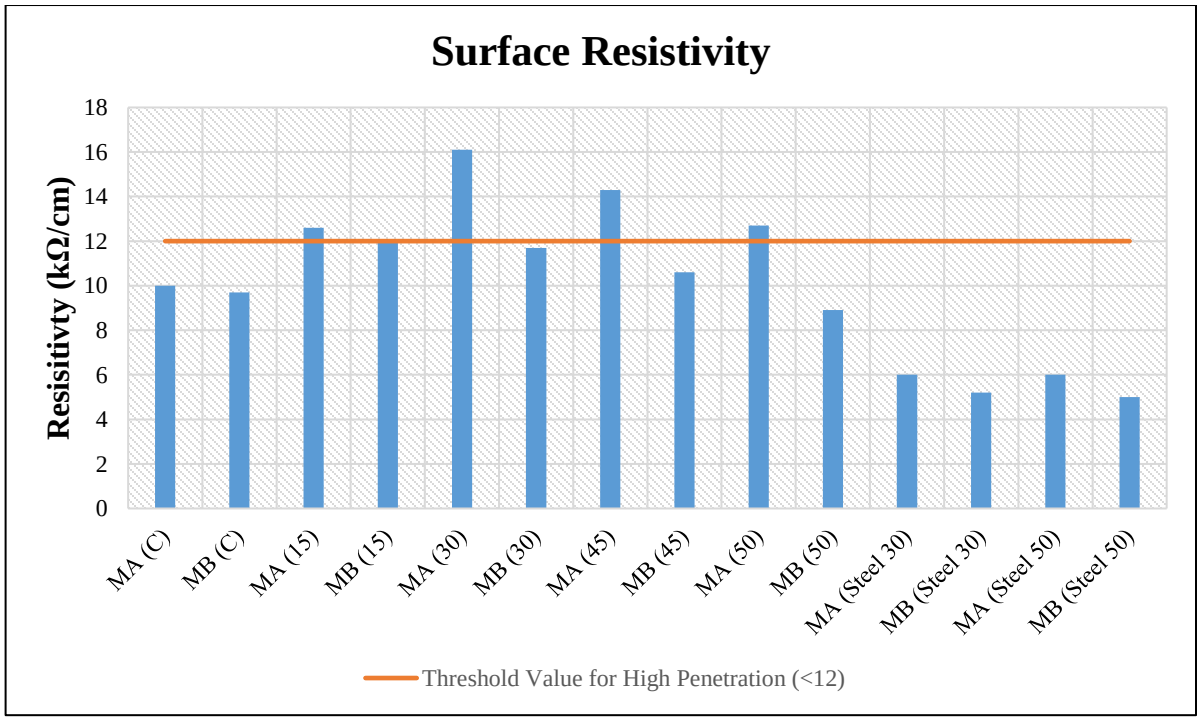

Figure 4-12: Surface Resistivity Graph

The results for measuring chloride ion penetrability can be seen in Table 4-3, where a low resistivity value (<12 kΩ/cm) indicates a high chloride ion penetrability.

Table 4-3: Surface Resistivity Test

Surface Resistivity Test	
Chloride Ion Penetration	**Electrical Resistivity (kΩ/cm)**
High	<12
Moderate	12-21
Low	21-37
Very Low	37-254
Negligible	>254

As can be seen from Figure 4-12, the addition of basalt fibers shows a decrease in chloride ion penetrability (>12 kΩ/cm) for all MA mixtures and a decrease in chloride ion penetrability up to a fiber volume of 0.30% for MB samples. The reason as to why 0.45 and 0.50% BF by volume did not provide higher values for MB samples may be attributed to the higher porosity attained from the increase in w/c ratio as well as fibers increasing voids during mixing and distribution of fibers may have been affected due to the higher fiber volume. Although balling of fibers was not experienced, higher fiber volumes affect distribution of fibers which decreases its efficiency. The highest improvement was for Group I is MA (30) with an increase of 61% chloride ion penetration resistance and for Group II is MB (45) with an increase of 47% chloride ion penetration resistance. As expected MA values are higher than MB due to the increase in w/c ratio and as can be seen, a fiber volume of 0.30% provides the highest improvement for BFRC samples. On the other hand, the use of steel fibers increased the chloride ion penetration resistance. This is due to the material properties of steel fibers and the interaction of steel fibers to be more susceptible to chloride attacks. The highest decrease in chloride ion penetrability resistance for SFRC was experienced by MB (Steel 50) with a decrease of 48.45%.

The effects of the addition of fibers on the chloride ion penetrability of FRC were investigated and are listed below:

1) The addition of fibers increased overall chloride ion penetrability resistance for both Group I (MA) and Group II (MB), with the exception of MB (50).
2) The highest chloride ion penetrability resistance increase experienced in Group I is by MA (30) with an increase of 61% and for Group II is by MB (15) with an increase of 23.71%.
3) As expected, an increase in w/c ratio reduces the effectiveness of enhancing the chloride ion penetrability resistance.
4) As expected, the use of steel fibers showed a decrease in chloride ion penetrability resistance.
5) The highest decrease in chloride ion penetrability resistance for SFRC was by Group II MB (Steel 50) with a decrease of 48.45%

CHAPTER 5: RAPID MACROCELL CORROSION EVALUATION TEST

5.1 INTRODUCTION

Corrosion of concrete reinforcement has been a major problem for concrete structures, especially concrete bridges that are continuously exposed to deicing chemicals. Various methods have been developed to reduce the damage caused by corrosio such as: implementing epoxy coated bars, galvanized bars, and implementing metal claddings to provide protection to the reinforcing steel members against corrosion. Corrosion performance evaluation of reinforcing steel embedded in concrete has typically been investigated by ASTM G 109, but this test is labor intensive and time consuming [94].

To address such problems, an experimental corrosion evaluation test was developed at the University of Kansas, under the Strategic Highway Research Program (SHRP), called the rapid macrocell test. The test consists of a galvanic cell, which is made up of two electrodes, the anode and the cathode, placed in two separate containers immersed in simulated concrete pore solution to simulate the top and bottom reinforcement mats of a bridge deck. The potential difference between the anode and cathode causes current flow and corrosion to occur. The current flow through the containers is measured by measuring voltage drop through resistors and is used to calculate the rate of metal loss using Faraday's law, see Equation 3.

$$m = \frac{(i * a)}{(n * F * D)} \tag{3}$$

Where:

m = Corrosion rate (μm/yr)

i = Current density of the macrocell (mA/cm^2)

a = Atomic weight of the metal (55.84 grams/gram-atom, for iron)

n = number of ion equivalents exchanged (for iron n=2; $Fe \rightarrow Fe^{++} + 2e^{-}$)

F = Faraday's constant (96,500 coulombs/equivalent)

D = Density of the metal (7.87 grams/cm^3, for iron)

The way a galvanic cell works is through a shift in energy, called the potential, between electrodes. In this case it is the different concentrations of chloride ions in the concrete pore solution. This shift in energy initiates the electrochemical process of oxidation and reduction reactions. Oxidation occurs at the positively charged electrode, called the anode; reduction occurs at the cathode, where electrons flow through due to the potential drop occurring at the anode. The voltage drop reading taken through this electrochemical process is used to monitor the corrosion rate of the macrocell.

Aside from measuring the corrosion rate, a second reading is also used to evaluate the corrosion state of the steel. This reading is the open circuit potential and is measured with respect to a standard reference electrode; in this study it is a saturated calomel electrode (SCE). The corrosion state of the reinforcement can be classified as passive, active, or indeterminate, depending on the difference in potential between the reinforcement and the reference electrode. The output current potential is measured with a voltmeter, measuring the voltage drop between the reference electrode and the reinforcement at the half-cell.

5.2 EXPERIMENTAL PROGRAM

In this section, the details of the experimental program conducted to evaluate the rapid macrocell test at the Buchanan Engineering Laboratory at the University of Idaho (UI) are discussed and reported. The aim of the test is to evaluate the effects basalt fiber have on the corrosion rate properties of the mortar mixtures. The study was done with varying basalt fiber volumes of 0%, 0.15%, 0.30%, 0.45% and 0.50% by total volume, utilizing two different water-to-cement ratios (w/c) of (0.35, 0.40) and comparing them to conventional mortar mixtures. The mix designs can be seen in Table 5-1.

Table 5-1: Mortar Mix Design

	Control Mixtures		**Basalt Fiber Mortar Mixtures**							
Material	MA (C)	MB (C)	MA (15)	MB (15)	MA (30)	MB (30)	MA (45)	MB (45)	MA (50)	MB (50)
Cement (Kg/m^3)	1506	1506	1506	1506	1506	1506	1506	1506	1506	1506
(lbs/yd^3)	2538	2538	2538	2538	2538	2538	2538	2538	2538	2538
F.A. (Kg/m^3)	1281	1281	1281	1281	1281	1281	1281	1281	1281	1281
(lbs/yd^3)	2160	2160	2160	2160	2160	2160	2160	2160	2160	2160
Water (Kg/m^3)	526	602	526	602	526	602	526	602	526	602
(lbs/yd^3)	888	1015	888	1015	888	1015	888	1015	888	1015
Fibers (Kg/m^3)	0.0	0.0	4.05	4.05	8.10	8.10	10.8	10.8	13.5	13.5
(lbs/yd^3)	0.0	0.0	6.83	6.83	13.7	13.7	18.2	18.2	22.7	22.7
HRWA (L/m^3)	0.0	0.0	0.60	0.50	0.60	0.50	0.60	0.50	0.62	0.62
(gal/yd^3)	0.0	0.0	0.12	0.10	0.12	0.10	0.12	0.10	0.13	0.13

*Mixture ratio 1:3; cement: sand

*Total volume per batch is of 0.045 ft^3

All of the test specimens had the necessary equipment and instruments to measure and record data from the experiment, but due to limitations in steel fibers such specimens were not cast and were not included in this study. The study followed report FHWA/TX-09/0-4825-1 [95] procedures for casting and testing with necessary changes being included and noted.

5.2.1 Materials

A Type I/II Portland cement with a specific gravity of 3.15 and conforming to the requirements of the ASTM C150, "Standard Specification for Portland Cement" [82] was used in the development of all mixtures in this study. Natural sand was used as fine aggregate (FA). Moisture absorption and specific gravity for fine aggregate were determined in accordance to ASTM C128, "Standard Test Method for Relative Density (Specific Gravity) and Absorption of Fine Aggregate" [84]. The fine aggregate had a relative specific gravity (SSD) of 2.683, absorption of 4.03%, and a fineness modulus of 2.93. A high range water reducing admixture (HRWA) utilizing Sika's 'ViscoCrete®4100' conforming to the requirements for ASTM C 494 Types A and F was also used in the mortar mixtures. The recommended dosages are between 325-780 mL/100kg (5-12 fl oz. /100 lbs) of cementitious materials. The basalt fibers were provided by Deutsche Basalt Faser GmbH and can be seen in Figure 3-1.

Three steel #5 reinforcement bars, with lengths of 5 inches were used per each macrocell test. A two-part high viscosity epoxy was used to coat the sections where steel specimens protruded from the mortar. The wire used to connect the specimens was a 16 gauge wire that was also connected to a 10 ohm resistor and a switch. A salt bridge was used to connect the anode and cathode electrodes, which was made of agar, KCL (Potassium Chloride), and distilled water. Concrete pore solutions were prepared by using NaOH (Sodium Hydroxide), KCL (Potassium Chloride) and NaCL (Sodium Chloride) for the anode electrode. Scrubbed air was obtained by passing pressurized air through a 1 M sodium hydroxide solution. Broken mortar samples were also used to fill the anode and cathode containers using the same mortar mixtures. A saturated calomel electrode (SCE) was used to monitor the output current potential and a voltmeter was used to measure voltage drop readings. The material properties of the materials mentioned are listed in Table 5-2 and can also be seen in Appendix B.

Table 5-2: Rapid Macrocell Test Material Properties

Material	Properties
Portland Cement (C)	Relative Density: 3.15
Natural Sand (FA)	Relative Density: 2.683
	Absorption: 4.03 %
	Fineness Modulus: 2.93
	Graded in Accordance with ASTM C 33
Basalt Fibers (BF)	Relative Density: 2.70
	Fiber Length: 24.13 mm (0.950”)
	Diameter: 0.60 mm (0.0235”)
	Aspect Ratio: 40
High-Range Water Reducing Admixture (HRWA) (Sika Viscocrete-4100)	Relative Density: 1.08
Normal Tap Water (W)	Density at 24°C (75.2 °F): 997.28 Kg/m^3 (62.3 lb/ft^3)
Steel Bar Reinforcement	Nominal Diameter: 15.875 mm (0.625”)
	Length: 127 mm (5”)
Stainless Steel Screws	Dimensions: No.6 X 3/8”
Specimen Mold	Height: 101.6 mm (4”)
	Width: 40.6 mm (1.6”)
Specimen Containers	Height: 101.6 mm (4”)
	Width: 152.4 mm (6”)
Two-Part High Viscosity Epoxy (J-B Weld Original Cold Weld)	Strength: 3960 Psi
	Set Time: 4-6 Hours
	Cure Time: 15-24 Hours
	Cure Color: Dark Grey
Electrical Wire	Wire Gauge: 16
Resistor	Ohm: 10
Switch (GB Toggle Switch)	Type: Toggle Switch GSW-13
Salt Bridge Tube (GSC International)	Length: 100 mm (3.94”)

	Type: U-Shaped Borosilicate Glass Drying Tube
Reference Electrode	Type: SCE (Saturated Calomel Electrode)
	Model: STREF2 Model
Voltmeter	Model: Fluke 77 III Multimeter

5.2.2 Test Set-Up

Steel reinforcement was cut to obtain 5-in (127mm) long specimens which were cleaned in preparation to casting. A 0.6 in. band of a two-part high viscosity epoxy was applied on the steel reinforcement centered on the protruding steel section. This coating was applied to prevent accelerated corrosion of steel specimens due to galvanic corrosion at the section where they protrude from the mortar, See Figure 5-1.

Figure 5-1: (Left) Steel Reinforcement, (Right) Two Part Epoxy Applied on Reinforcement

Three mortar specimens were cast with a No. 5 (No. 16M) steel reinforcement bar protruding from the center of the mold with a bottom cover of 1 inch, see Figure 5-2.

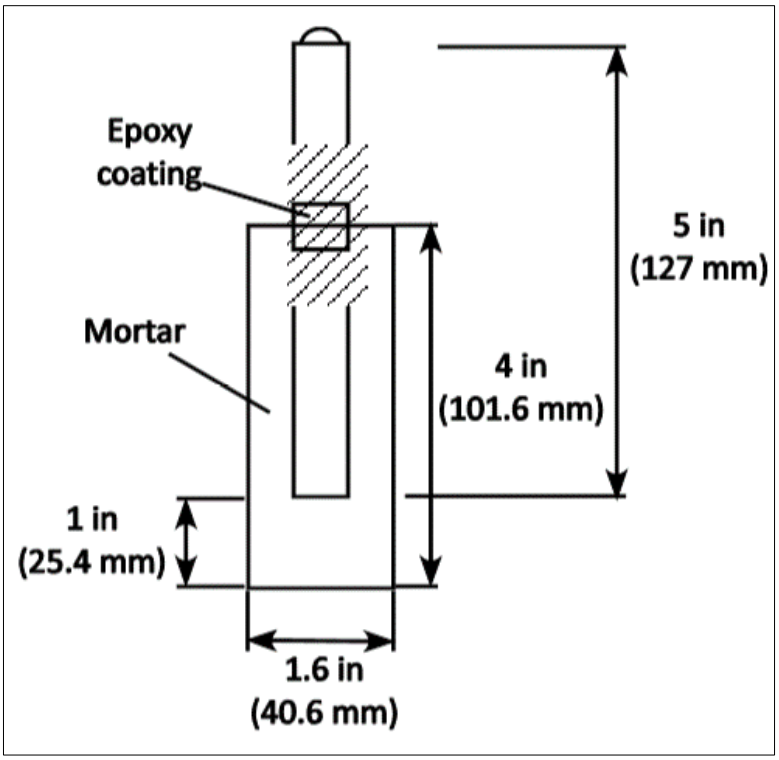

Figure 5-2: Mortar Covered Steel Specimen [95]

A rotatory drum mixer was used to mix all mortar ingredients in accordance with the ASTM C 305 “Standard Practice for Mechanical Mixing of Hydraulic Cement Pastes and Mortars of Plastic Consistency” [96]. Molds were cast with three additional containers of mortar mix, which was pre-cut to dimensions of <2in. to serve as mortar fill, see Figure 5-3.

Figure 5-3: Macrocell Specimens & Mortar Fill

All prepared mortar samples were covered and left in plastic molds undisturbed for 24 hours. Subsequently, they were unmolded and stored in 95% or higher humidity until the day of testing, see Figure 5-4.

Figure 5-4: (Left) Demolded Macrocell Sample; (Right) Curing of Samples

Once samples were cured, the samples were taken out from the curing room, dried, labeled and connected electrically as shown in Figure 5-5. Samples were also covered with protective tape for protective purposes, both electrically and to limit corrosion from other sources.

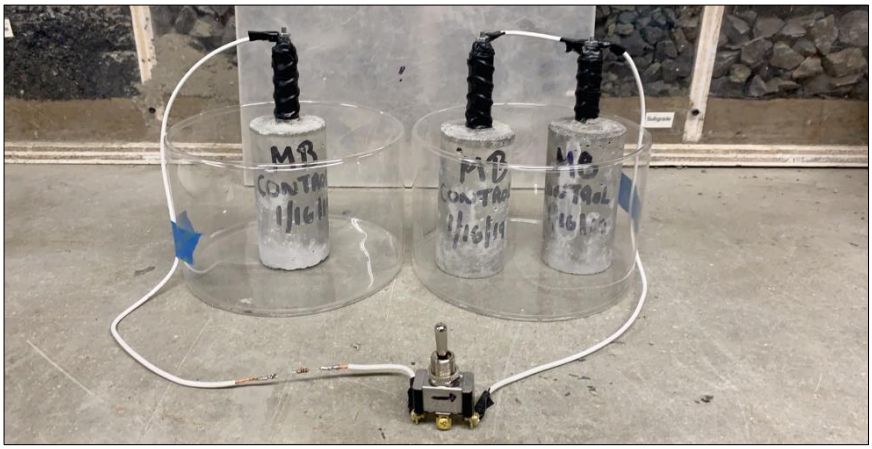

Figure 5-5: Macrocell Electrical Set-up

The macrocell electrical set-up consists of the following wire length dimensions:

- Cathode Top Connection: 3-3.2 in. wire length
- Cathode to switch: 15-15.5 in. wire length
- Switch to Resistor: 3 in. wire length
- Resistor to Anode Top Connection: 15 in. wire length

Once the electrical set-up was set, the concrete pore solutions were prepared as follows:

- Anode Macrocell: 18.81 g KOH, 17.87 g NaOH, 974.8 g Distilled Water, 45.6 g NaCl
- Cathode Macrocell: 18.81 g KOH, 17.87 g NaOH, 974.8 g Distilled Water

All solutions are per 1L of solution with anode containers having a 1.6M NaCl solution and are made to fill the containers to a height of 3.72 inches. Alongside the pore solutions, the scrubbed air was also set-up with the following set-up and solutions, see Appendix B for figures:

- Container: Length (13 in.) x Height (6 in.)
- Bubbler: 5 in. Air Bubble Stone Disc Bubble Diffuser
- Connections: Plastic tubing, between cathodes about 1 in. connections
- Solution: 1M NaOH (40 g NaOH per 1000 g Distilled Water)
- Air Supply: Pressurized air at 40-60 KPa (10-15 psi)

The container was filled about ¾ full of solution and required maintenance of materials as well as replenishing of solution as water will evaporate with time.

5.2.3 Salt Bridge

A salt bridge is required to maintain electrical neutrality in the cell. Without a salt bridge, the solution of the half-cells will become imbalanced and the cell voltage will eventually drop to zero. The salt bridge allows for ions to migrate between the solutions to maintain an equal charge within the cell.

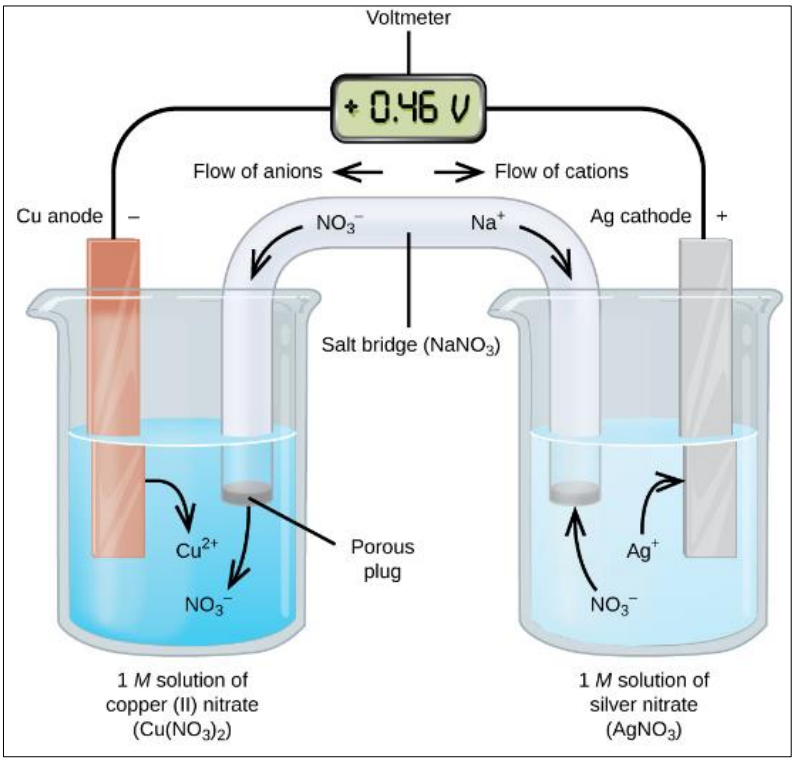

Figure 5-6: Salt Bridge Interaction Example [BC Open Textbooks]

The anode in the electrical circuit loses electrons, while the cathode gains electrons, and so a salt bridge is added to maintain electrical neutrality within the cell. The salt bridge acts as a pathway for ions to migrate from one solution to the other which allows for the redox reactions to continue. The salt bridge is made of a salt solution, usually KCL (Potassium Chloride) or NaCL (Sodium Chloride). The following materials were used to create the salt bridges in this study:

- 100 mm long U-Shaped Glass Tube

- 4.5 g of agar (Used to create semisolid gel)
- 30 g of KCL (Potassium Chloride)
- 100 g Distilled Water

All the materials are heated on a hot plate and stirred continuously until solution is melted. After melting, agar solution is placed into the tubes, keeping the ends higher than the center of the tube to prevent discharge. Tubes are placed in boiling water for 4 hours, keeping ends of the tubes out of the water. After removal from boiling water and after samples have cooled, the salt bridge is inspected for air bubbles and tested for conductivity using a (DC) power source connected to two beakers filled with a chloride solution. Typical life span of a salt bridge is three weeks, after which the tubes are cleaned and another set of salt bridges are made. If the gel solution starts to flow out into the test containers, then the test specimens must be removed, cleaned and replaced with new solutions.

Figure 5-7: Salt Bridge

Once all materials are set-up, solutions prepared and salt bridges prepared. The theoretical macrocell set-up can be seen in Figure 5-8. The test is performed by taking two readings,

voltage drop between anode and cathode; and voltage drop between reference electrode and anode, also known as the open current potential (OCP). Data is collected three times a week for a minimum of 100 days. Macro cell corrosion current is determined by measuring the voltage drop across the resistor by connecting the positive lead of a voltmeter to the anode sample and the negative lead to the cathode sample. After taking the voltage drop readings, the switches are turned off and a waiting period of two hours is suggested. After the waiting period, the OCP readings are taken using the voltmeter and saturated calomel electrode. After collection of the OCP readings, the switches are turned back on until the next set of readings.

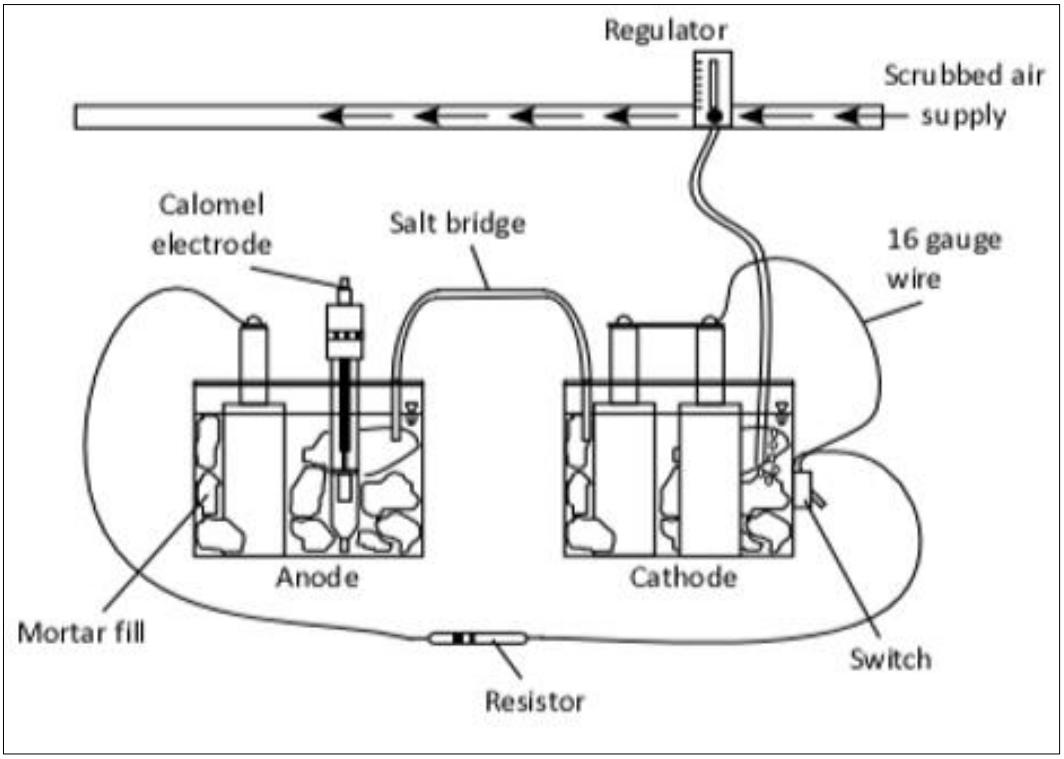

Figure 5-8: Theoretical Rapid Macrocell Set-Up [95]

Due to limitations of the lab and limitations on materials, the set-up for this study utilized scrubbed air supply from bubbling of 1M NaOH solution in a container with a bubbler device and feeding the scrubbed air through a series of tubes to the cathode containers in the experiments. The final set-up for this study can be seen in Figure 5-9.

Figure 5-9: Experimental Rapid Macrocell Set-Up

5.3 EXPERIMENTAL RESULTS

The deterioration of reinforced concrete due to corrosion of steel reinforcement has been studied and monitored by various standardized tests. The corrosion rate gives an indication of the corrosion performance of steel in concrete which allows for evaluation of different corrosion protection methods. Such corrosion protection methods have included increased cover depths, lower permeability concrete, corrosion inhibitors, epoxy coated steel, and many others [95]. In this study the effects of including basalt fibers in various fiber volumes and different w/c ratios were investigated to evaluate the corrosion performance of the mixtures.

Previous studies on the chloride penetration resistance of BFRC provided an unclear answer as to the effect BF have on the corrosion performance of BFRC. Some studies showed that the addition of BF improved the resistance to chloride penetration, but with the addition of cementitious materials such as fly ash, or silica fume. Other studies have shown that the addition of fibers decreases resistance to chloride penetration and can even increase internal microcracks and pores within the matrix, which accelerate corrosion activity. The test in this study is important, since no supplementary cementitious materials were included and the effects of basalt fiber have not been tested with the rapid macrocell test. The addition of BF was assumed to improve the corrosion resistance due to the improved durability properties and also due to the non-corrosive properties of basalt fibers. The results for the corrosion rate of the study and open circuit potential can be seen in Figure 5-10 and Figure 5-11, respectively. Samples were also inspected once tests were terminated and can be seen in Appendix-B.

5.3.1 Corrosion Rate

As can be seen from Figure 5-10, the addition of fibers into the mix increases corrosion rates. The maximum corrosion rate exhibited is around 14 µm/yr by MB (50) and varies around 8 and 12 µm/yr. The rates for the control samples maintain a corrosion rate close to 0 for about 57 days for MA and 36 days for MB, after which rates increase to around 2 to 4 µm/yr for MA and around 5 to 8 µm/yr for MB. Results show that MA (15) maintains a relatively low corrosion rate, close to 0 µm/yr, for around 55 days, but due to insufficient data it is not clear if the trend would continue as low or if it would follow the trend of MA control, as MB (15) followed the trend of MB control at a shorter time period. As can be seen, MB samples tend to stabilize around 8 and 10 µm/yr, with the exception of MB (50), whereas MA samples stabilize around 6 to 4 µm/yr.

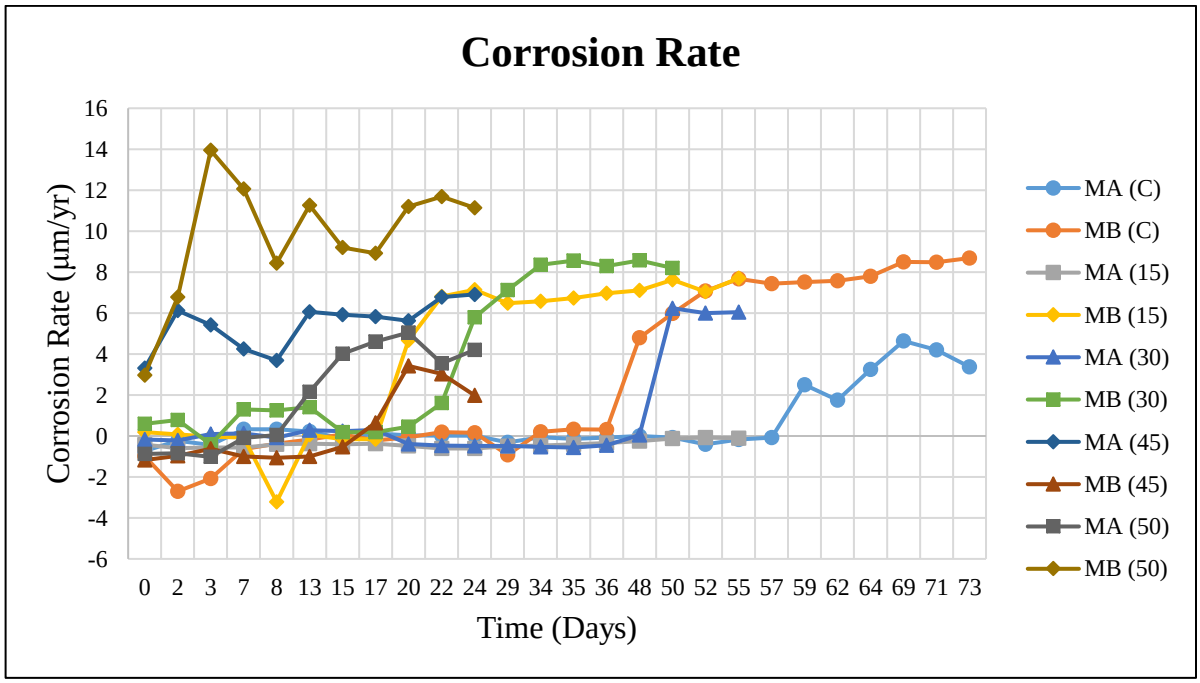

Figure 5-10: Corrosion Rate Graph

5.3.2 Open Circuit Potential

The open circuit potential (OCP) readings were measured with respect to a saturated calomel electrode, see Appendix-B. OCP readings were taken after voltage drop readings were recorded, after which all switches were turned off and a two hour waiting period was taken before readings were taken. Switches were turned on again after readings were taken and left

on until next set of readings. Data was collected weekly and then three times a week. Potential of corrosion activity is evaluated by ASTM C 876 guidelines, see Table 5-3.

Table 5-3: Corrosion Interpretations (ASTM C 876)

Half-Cell Potential Readings (V)		
CSE[1]	SCE[2]	Corrosion Activity
>-0.200	>-0.125	Greater than 90% probability of no corrosion
-0.200 to -0.350	-0.125 to -0.275	An increasing probability of corrosion
<-0.350	<-0.275	Greater than 90% probability of corrosion

[1]Copper-Copper Sulfate Electrode, [2]Saturated Calomel Electrode

OCP readings indicate that the addition of basalt fibers increases the potential for corrosion with the increase in fiber volume. As can be seen from Figure 5-10, MB (50) OCP readings drop below -0.275 V and maintain a reading of around -0.500 V indicating a potential for corrosion within the first three weeks. MA (45) is another sample that displays a similar corrosion potential, with OCP values dropping below -0.275 V within the first three weeks. On the other hand, MA control samples stay around -0.150 V for about eight weeks before dropping to around -0.275 V. A similar trend is seen for MB control samples, but with corrosion potential dropping below -0.275 V after six weeks period. As can be seen, the addition of fibers reduces the time period at which samples experience corrosion potentials below -0.275 V. As explained with corrosion rate results, OCP results are also difficult to interpret as the testing period was not adequate and not enough data was gathered for all samples.

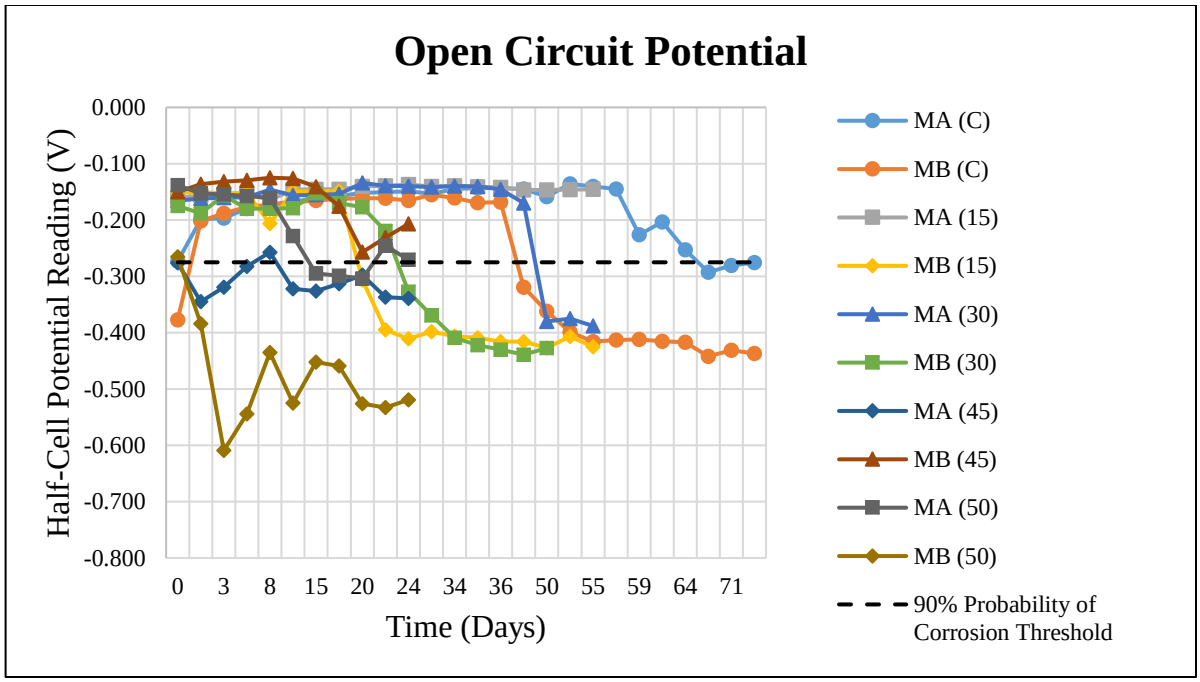

Figure 5-11: Open Circuit Potential Graph

The effects of the addition of basalt fibers on the corrosion evaluation of steel reinforcement covered mortar samples were investigated and are listed below:

1) The addition of basalt fibers increased overall corrosion rates of all mixtures.
2) The highest corrosion rate experienced in Group I is by MA (45) with a corrosion rates around 4 to 7 μm/yr and for Group II is by MB (50) with a corrosion rates around 8 to 12 μm/yr.
3) The highest OCP experienced in Group I is by MA (45) with OCP around -0.350 V within the first three weeks and for Group II is by MB (50) with OCP between -0.600 V and -0.500 V within the first three weeks.
4) An increase in w/c ratio increases corrosion rates, decreases time of corrosion experienced by samples and decreases time of corrosion potential of samples to drop below -0.275 V threshold.

CHAPTER 6: SUMMARY AND CONCLUSIONS

6.1 FRESH PROPERTIES OF FRC

All the concrete mixtures met the required slump target range of 6 in. ± 2 in. with no signs of bleeding, segregation or balling of fibers. Control mixtures did not require any HRWA and the amount of HRWA required for FRC mixtures increased with the increase of fiber volume fractions. The SFRC mixtures required less HRWA when compared to the same mixtures containing basalt fibers, which can be attributed to material characteristic of steel fibers as well as the increased surface area when compared to basalt fibers. Overall, the results indicate that as fiber volume increases and as w/c ratio increases, slump decreases and HRWA amounts required increase.

Concrete unit weight of mixtures showed an increase as fiber volumes increased up to a fiber volume of 0.30%, after which unit weight values decreased. SFRC mixtures showed increased unit weight values at the same fiber volumes as basalt, which may be attributed to the higher density of the material. Overall results indicate that as fiber volumes increase, unit weight values increase until an optimum fiber volume is reached. In this study, the optimum fiber volume is recommended to be 0.30% for BFRC mixtures.

6.2 MECHANICAL PROPERTIES OF FRC

All the mixtures for both Groups I and II have an average 28-day compressive strength greater than the average specified compressive strength (5075 psi) for typical fiber reinforced concrete mixtures. The addition of fibers decreases the compressive strength at 28 days, with the exception of MB (30) which showed an increase of 0.98% compared to MB (C). The early age (7-day) compressive strengths, on the other hand, tend to increase with fiber volume for Group I and decrease for Group II. The addition of steel fibers displayed similar compressive strengths when comparing to similar fiber volumes used for basalt fiber mixtures. Overall results display a decrease in 28-day compressive strength as fiber volumes increase, but show an overall increase in early age compression when a lower w/c was used.

The tensile strength of both mixture Groups I and II showed an increase as fiber volume fraction increased, which is attributed to the bridging interaction the fibers provide in reducing

micro and macro-cracks from expanding. The use of steel fibers displayed a lesser impact when compared to the same basalt fiber volume fraction. Overall results displayed a significant increase in tensile strength for both BFRC and SFRC mixtures.

Flexural strengths for all FRC mixtures increased significantly with the increase in fiber volume. However, 0.50% fibers by volume did not provide the highest flexural strength which is attributed to inefficiency in fiber distribution and the increased cementitious material required to coat both fibers and aggregates. The use of steel fibers displayed similar flexural strengths at the same basalt fiber volume fractions. Overall results displayed a significant increase in flexural strength for both BFRC and SFRC mixtures.

The ARS for both mixture Groups I and II displayed an increase as fiber volumes increased. This is attributed to the bridging interaction mentioned, as well as the increased ductility provided by the inclusion of fibers.

Overall results displayed increased mechanical properties when fibers are used, basalt or steel, with the exception of 28-day compressive strength. The optimum fiber volume to increase overall mechanical properties seems to be around 0.30-0.45%, which would also provide increased early age compressive strength.

6.3 DURABILITY PROPERTIES OF FRC

Overall, the ultimate drying shrinkage strains (microstrain) decreased with the increase in fiber volumes. The results indicated SFRC performed considerably better when compared to the same BFRC fiber volumes. The increased w/c ratio also displayed a decreased in shrinkage strain values, which is attributed to the increased water available during the cement hydration process allowing the concrete to maintain its volume for a longer period of time. The results display an initial increase in shrinkage strains which is attributed to the 7-day moist curing period, after which the specimens were set to air dry. Overall results showed a decrease in ultimate drying shrinkage strains for both SFRC and BFRC with the increase in fiber volume as well as an increase in w/c ratio.

Chloride ion penetrability resistance results displayed an overall increase with the increase in basalt fiber volumes. SFRC mixtures displayed a decrease in chloride ion penetrability resistance, which was expected because the material characteristics of steel fibers are more

susceptible to corrosion. Overall results indicated that a fiber volume of 0.30%, for basalt fibers, as well as a lower w/c ratio provide improved chloride ion penetrability resistance properties.

The corrosion evaluation results showed an increase in corrosion rates with the increase of basalt fiber volumes. The results also showed a faster potential for corrosion when fiber volumes increased. The increase in w/c ratio increased corrosion rates and also decreased the time samples experienced potential for corrosion. The results of this study are important, but interpretation of the results is not as clear as no data on the addition of fibers have been studied for this specific test and the test time of 100 days was not achieved. Overall, results gathered in this study showed that corrosion of steel reinforcement accelerated when basalt fibers were added.

Overall results displayed improved durability properties for unrestrained drying shrinkage and chloride ion penetrability with the increase in fiber volume. Basalt fibers are more suited towards improving chloride ion penetrability resistance when a fiber volume of 0.30% and a lower w/c ratio is used. Steel fibers on the other hand, are better used to reduce the shrinkage strains of the concrete when higher fiber volumes are used with a higher w/c ratio.

6.4 GENERAL CONCLUSIONS FOR BFRC

This research provides the results from an experimental study investigating the effects of basalt fibers on the fresh, mechanical, durability and corrosion properties of BFRC. The following observations and conclusions can be drawn from the results of this investigation.

1. Slump target values can be achieved with an increase in HRWA of about 11.33 ml/ft^3 per 10% fiber increase, allowing higher workability of the mixtures without experiencing bleeding or segregation.
2. 28-day compressive strengths decrease with the increase in fiber volume, but could be used to enhance early-age (7-day) compressive strengths with a low w/c ratio.
3. Utilizing a fiber volume of 0.30% seemed to optimize the mixtures as it displayed an overall improvement in mechanical properties.
4. Average residual strengths as well as shrinkage strain values are improved with the increase in fiber volumes.

5. Chloride ion penetrability resistance is improved with the addition of basalt fibers and a fiber volume of 0.30% displayed the most improvement.
6. Corrosion rates and potential for corrosion increase as fiber volumes increase.

In conclusion, the use of basalt fibers reduces slump values, but with the right amount of HRWA slump target values can be achieved. The use of basalt fibers also improves tensile, flexural and average residual strength, but reduces compressive strength at 28-days. Durability properties, unrestrained drying shrinkage and chloride ion penetrability, are also improved with the addition of basalt fibers. Corrosion rates and potential for corrosion are negatively affected with the addition of basalt fibers. It is suggested to use a fiber volume of 0.30% to optimize the overall improvement of the mixtures, as this study has shown.

6.5 RECOMMENDATIONS FOR FUTURE RESEARCH FOR BFRC

1. Investigate higher fiber volumes (>1%) as well as different fiber aspect ratios.
2. Investigation of mixtures utilizing a blend of different fiber types.
3. Further research on corrosion monitoring as well as impact resistance tests.
4. Investigate durability issues such as freeze-thaw, chloride attack, and other acid attacks.

REFERENCES

[1] ACI Committee 544. State-of-the-art report on fiber reinforced concrete (ACI 544.1R-96). American Concrete Institute, Farmington Hills; 2002. p. 66

[2] Yakhlaf, M. (2015). Fresh and Mechanical Properties of Basalt Fiber Reinforced Concrete. 10.13140/RG.2.1.3585.2888.

[3] Iyer, P., Kenno, S. Y., & Das, S. (2015). Mechanical properties of fiber-reinforced concrete made with basalt filament fibers. Journal of Materials in Civil Engineering, 27(11), 04015015.

[4] El-Gelani, A. M., High, C. M., Rizkalla, S. H., & Abdalla, E. A. (2018). Effects of Basalt Fibres on Mechanical Properties of Concrete. In MATEC Web of Conferences (Vol. 149, p. 01028). EDP Sciences.

[5] Kosmatka, S. H., Kerkhoff, B., & Panarese, W. C. (2002). Design and control of concrete mixtures (Vol. 5420, pp. 60077-1083). Skokie, IL: Portland Cement Association.

[6] Pareek, Krishan & Saha, Purna. (2019). Basalt Fiber and Its Composites: An Overview.

[7] Ralph, C., Lemoine, P., Summerscales, J., Archer, E., & McIlhagger, A. (2019). The relationship between the chemical, mechanical and geometrical properties of basalt fibre.

[8] Deák, T., & Czigány, T. (2009). Chemical Composition and Mechanical Properties of Basalt and Glass Fibers: A Comparison. Textile Research Journal, 79(7), 645–651. doi: 10.1177/0040517508095597

[9] Kumbhar, Vishal. (2014). An overview: basalt rock fibres-new construction material. Acta Eng Int. 2. 11-18.

[10] Þórhallsson, Eyþór & Erlendsson, Jon & Erlendsson, Ögmundur. (2013). Basalt fiber introduction.

[11] Ralph, C., Lemoine, P., Summerscales, J., Archer, E., & McIlhagger, A. (2019). The relationship between the chemical, mechanical and geometrical properties of basalt fibre.

[12] Seydibeyoğlu, M. Ö, Mohanty, A. K., & Misra, M. (Eds.). (2017). Fiber Technology for Fiber-Reinforced Composites. Woodhead Publishing.

[13] Patil, R. K., & Kulkarni, D. B. (2014). Comparative Study Of Effect Of Basalt, Glass And Steel Fiber On Compressive And Flexural Strength Of Concrete. International Journal of Research in Engineering and Technology, 03(06), 436-438. doi:10.15623/ijret.2014.0306080

[14] Yakhlaf, M. (2015). Fresh and Mechanical Properties of Basalt Fiber Reinforced Concrete. 10.13140/RG.2.1.3585.2888.

[15] Jiang, C., Fan, K., Wu, F., & Chen, D. (2014). Experimental study on the mechanical properties and microstructure of chopped basalt fibre reinforced concrete. Materials & Design, 58, 187–193. doi: 10.1016/j.matdes.2014.01.056

[16] K. Kirthika, S & Singh, SK. (2018). Experimental Investigations on Basalt Fibre-Reinforced Concrete. Journal of The Institution of Engineers (India): Series A. 99. 10.1007/s40030-018-0325-4.

[17] Singh, SK & k kirthika, s & Maruthupandian, Surya. (2018). Durability Studies on Basalt Fibre Reinforced Concrete. Indian Concrete Journal. 92.

[18] Kayali, O. (2016). Sustainability of fibre composite concrete construction. Sustainability of Construction Materials, 539–566. doi: 10.1016/b978-0-08-100370-1.00021-4

[19] ACI Committee 544. State-of-the-Art Report on Fiber Reinforced Concrete. Farmington Hills, MI, USA: American Concrete Institute, 1996. ACI 544.1R-96.

[20] Romualdi, J.P., Batson, G.B., 1963. Reducing the fiber spacing increases the tensile strength- mechanics of crack arrest in concrete. Proc. ASCE J. Eng. Mech. Div. 89, 147–168.

[21] Romualdi, J. P., & Mandel, J. A. (1964, June). Tensile strength of concrete affected by uniformly distributed and closely spaced short lengths of wire reinforcement. In Journal Proceedings (Vol. 61, No. 6, pp. 657-672).

[22] Sim, J., Park, C., & Moon, D. Y. (2005). Characteristics of basalt fiber as a strengthening material for concrete structures. Composites Part B: Engineering, 36(6-7), 504–512. doi: 10.1016/j.compositesb.2005.02.002

[23] Iyer, P., Kenno, S. Y., & Das, S. (2015). Mechanical Properties of Fiber-Reinforced Concrete Made with Basalt Filament Fibers. Journal of Materials in Civil Engineering, 27(11), 04015015–1-04015015–8. doi: 10.1061/(asce)mt.1943-5533.0001272

[24] Xin Yang, Yong & Lian, Jie. (2011). Basalt Fiber Reinforced Concrete. Advanced Materials Research. 194-196. 1103-1108. 10.4028/www.scientific.net/AMR.194-196.1103.

[25] Yao, W., Li, J., & Wu, K. (2003). Mechanical properties of hybrid fiber-reinforced concrete at low fiber volume fraction. Cement and concrete research, 33(1), 27-30.

[26] Abbas, U. (2013). Materials development of steel-and basalt fiber-reinforced concretes (Master's thesis, Institutt for konstruksjonsteknikk).

[27] Halvaei, M., Jamshidi, M., & Latifi, M. (2016). Effect of fiber geometry and tenacity on the mechanical properties of fine aggregates concrete. Journal of Industrial Textiles, 45(5), 1083-1099.

[28] Gettu, R., Gardner, D. R., Saldivar, H., & Barragán, B. E. (2005). Study of the distribution and orientation of fibers in SFRC specimens. Materials and Structures, 38(1), 31-37.

[29] Yazıcı, Ş., İnan, G., & Tabak, V. (2007). Effect of aspect ratio and volume fraction of steel fiber on the mechanical properties of SFRC. Construction and Building Materials, 21(6), 1250-1253.

[30] Altun, F., Haktanir, T., & Ari, K. (2007). Effects of steel fiber addition on mechanical properties of concrete and RC beams. Construction and Building Materials, 21(3), 654-661.

[31] Błaszczyński, T., & Przybylska-Fałek, M. (2015). Steel fibre reinforced concrete as a structural material. Procedia Engineering, 122, 282-289.

[32] Abbass, W., Khan, M. I., & Mourad, S. (2018). Evaluation of mechanical properties of steel fiber reinforced concrete with different strengths of concrete. Construction and Building Materials, 168, 556-569.

[33] Olivito, R. S., & Zuccarello, F. A. (2010). An experimental study on the tensile strength of steel fiber reinforced concrete. Composites Part B: Engineering, 41(3), 246-255.

[34] Thomas, J., & Ramaswamy, A. (2007). Mechanical properties of steel fiber-reinforced concrete. Journal of materials in civil engineering, 19(5), 385-392.

[35] Katzer, J. 2006. "Steel Fibers and Steel Fiber Reinforced Concrete in Civil Engineering". Pacific Journal of Science and Technology. 7(1):53-58.

[36] ASTM A820 / A820M-16, Standard Specification for Steel Fibers for Fiber-Reinforced Concrete, ASTM International, West Conshohocken, PA, 2016

[37] İskender, Muhammet & Karasu, Bekir. (2018). Glass Fibre Reinforced Concrete (GFRC). El–Cezeri Journal of Science and Engineering (EJCSE). 5. 136–162. 10.31202/ecjse.371950.

[38] Bunsell, A. R. (Ed.). (2018). Handbook of properties of textile and technical fibres. Woodhead Publishing.

[39] Wallenberger, F. T., Watson, J. C., & Li, H. (2000). Glass Fibers. PPG Industries. Inc., ASM International, Ohio, USA.

[40] Labib, W. A. (2018). Fibre Reinforced Cement Composites. Cement Based Materials, 31.

[41] Wang, Y. (1998). Toughness characteristics of synthetic fibre-reinforced cementitious composites. Fatigue & fracture of engineering materials & structures, 21(4), 521-532.

[42] Zheng, Z., & Feldman, D. (1995). Synthetic fibre-reinforced concrete. Progress in Polymer Science, 20(2), 185-210.

[43] Kaur, P., & Talwar, M. (2017). Different types of Fibres used in FRC. International Journal of Advanced Research in Computer Science, 8(4).

[44] Reis, J. M. L. (2006). Fracture and flexural characterization of natural fiber-reinforced polymer concrete. Construction and building materials, 20(9), 673-678.

[45] Toledo Filho, R. D., Scrivener, K., England, G. L., & Ghavami, K. (2000). Durability of alkali-sensitive sisal and coconut fibres in cement mortar composites. Cement and concrete composites, 22(2), 127-143.

[46] Beltran, M. S. (2011). Ductile cement-based composites with wood fibres (Doctoral dissertation, PhD Thesis, Delft University of Technology, The Netherlands).

[47] Chakar, F. S., & Ragauskas, A. J. (2004). Review of current and future softwood kraft lignin process chemistry. Industrial Crops and Products, 20(2), 131-141.

[48] Bajpai, P. (2011). Environmentally friendly production of pulp and paper. John Wiley & Sons.

[49] Behbahani, Hamid & Nematollahi, Behzad. (2011). Steel Fiber Reinforced Concrete: A Review.

[50] ACI Committee. (1988). Design considerations for steel fiber reinforced concrete (ACI 544.4 R-88). In American Concrete Institute.

[51] Fu, S. Y., & Lauke, B. (1996). Effects of fiber length and fiber orientation distributions on the tensile strength of short-fiber-reinforced polymers. Composites Science and Technology, 56(10), 1179-1190.

[52] Banthia, N., & Gupta, R. (2006). Influence of polypropylene fiber geometry on plastic shrinkage cracking in concrete. Cement and concrete Research, 36(7), 1263-1267.

[53] Alberti, M. G., Enfedaque, A., & Gálvez, J. C. (2016). Fracture mechanics of polyolefin fibre reinforced concrete: Study of the influence of the concrete properties, casting procedures, the fibre length and specimen size. Engineering Fracture Mechanics, 154, 225-244.

[54] Simões, T., Octávio, C., Valença, J., Costa, H., Dias-da-Costa, D., & Júlio, E. (2017). Influence of concrete strength and steel fibre geometry on the fibre/matrix interface. Composites Part B: Engineering, 122, 156-164.

[55] Singh, S., Shukla, A., & Brown, R. (2004). Pullout behavior of polypropylene fibers from cementitious matrix. Cement and Concrete Research, 34(10), 1919-1925.

[56] Deng, F., Ding, X., Chi, Y., Xu, L., & Wang, L. (2018). The pull-out behavior of straight and hooked-end steel fiber from hybrid fiber reinforced cementitious composite: Experimental study and analytical modelling. Composite Structures, 206, 693-712.

[57] Soulioti, D. V., Barkoula, N. M., Koutsianopoulos, F., Charalambakis, N., & Matikas, T. E. (2013). The effect of fibre chemical treatment on the steel fibre/cementitious matrix interface. Construction and Building Materials, 40, 77-83.

[58] Naaman, A. E., Namur, G. G., Alwan, J. M., & Najm, H. S. (1991). Fiber pullout and bond slip. I: Analytical study. Journal of Structural Engineering, 117(9), 2769-2790.

[59] Zīle, E., & Zīle, O. (2013). Effect of the fiber geometry on the pullout response of mechanically deformed steel fibers. Cement and concrete research, 44, 18-24.

[60] Löfgren, I. (2005). Fibre-reinforced Concrete for Industrial Construction-a fracture mechanics approach to material testing and structural analysis. Chalmers University of Technology.

[61] Zhou, B., & Uchida, Y. (2017). Relationship between fiber orientation/distribution and post-cracking behaviour in ultra-high-performance fiber-reinforced concrete (UHPFRC). Cement and Concrete Composites, 83, 66-75.

[62] Soroushian, P., & Lee, C. D. (1990). Distribution and orientation of fibers in steel fiber reinforced concrete. Materials Journal, 87(5), 433-439.

[63] Stähli, P., Custer, R., & van Mier, J. G. (2008). On flow properties, fibre distribution, fibre orientation and flexural behaviour of FRC. Materials and Structures, 41(1), 189-196.

[64] Şanal, İ., & Zihnioğlu, N. Ö. (2013). To what extent does the fiber orientation affect mechanical performance?. Construction and Building Materials, 44, 671-681.

[65] Laranjeira, F., Aguado, A., Molins, C., Grünewald, S., Walraven, J., & Cavalaro, S. (2012). Framework to predict the orientation of fibers in FRC: a novel philosophy. Cement and Concrete Research, 42(6), 752-768.

[66] Li, V. C. (1998). Engineered cementitious composites-tailored composites through micromechanical modeling.

[67] Branston, J., Das, S., Kenno, S. Y., & Taylor, C. (2016). Influence of basalt fibres on free and restrained plastic shrinkage. Cement and Concrete Composites, 74, 182-190.

[68] Gali, S., & Subramaniam, K. V. (2017). Evaluation of crack propagation and post-cracking hinge-type behavior in the flexural response of steel fiber reinforced concrete. International Journal of Concrete Structures and Materials, 11(2), 365-375.

[69] Barluenga, G., & Hernández-Olivares, F. (2007). Cracking control of concretes modified with short AR-glass fibers at early age. Experimental results on standard concrete and SCC. Cement and Concrete Research, 37(12), 1624-1638.

[70] Ramakrishnan, V., Wu, G. Y., & Hosalli, G. (1989). Flexural behavior and toughness of fiber reinforced concretes. Transportation Research Record, 1226, 69-77.

[71] Hao, Y., & Hao, H. (2013). Dynamic compressive behaviour of spiral steel fibre reinforced concrete in split Hopkinson pressure bar tests. Construction and Building Materials, 48, 521-532.

[72] Balaguru, P., & Dipsia, M. G. (1993). Properties of fiber reinforced high-strength semi-lightweight concrete. Materials Journal, 90(5), 399-405.

[73] Song, P. S., & Hwang, S. (2004). Mechanical properties of high-strength steel fiber-reinforced concrete. Construction and Building Materials, 18(9), 669-673.

[74] Aydin, A. C. (2007). Self compactability of high volume hybrid fiber reinforced concrete. Construction and Building Materials, 21(6), 1149-1154.

[75] Maalej, M., Hashida, T., & Li, V. C. (1995). Effect of fiber volume fraction on the off-crack-plane fracture energy in strain-hardening engineered cementitious composites.

[76] Soroushian, P., & Bayasi, Z. (1991). Fiber type effects on the performance of steel fiber reinforced concrete. Materials Journal, 88(2), 129-134.

[77] Chen, Y., Matalkah, F., Weerasiri, R. R., Balachandra, A. M., & Soroushian, P. (2017). Dispersion of fibers in ultra-high-performance concrete. Concrete International, 39(12), 45-50.

[78] ACI Committee 212. Report on Chemical Admixtures for Concrete (ACI 212.3R-16). American Concrete Institute, Farmington Hills; 2016. p. 76

[79] ASTM C494 / C494M-17, Standard Specification for Chemical Admixtures for Concrete, ASTM International, West Conshohocken, PA, 2017, www.astm.org

[80] ASTM C1017 / C1017M-13e1, Standard Specification for Chemical Admixtures for Use in Producing Flowing Concrete, ASTM International, West Conshohocken, PA, 2013, www.astm.org

[81] ACI Committee 544. Guide to Design with Fiber-Reinforced Concrete (ACI 544.4R-18). American Concrete Institute, Farmington Hills; 2018. p. 44

[82] ASTM C150 / C150M-19a, Standard Specification for Portland Cement, ASTM International, West Conshohocken, PA, 2019, www.astm.org

[83] ASTM C127-15, Standard Test Method for Relative Density (Specific Gravity) and Absorption of Coarse Aggregate, ASTM International, West Conshohocken, PA, 2015, www.astm.org

[84] ASTM C128-15, Standard Test Method for Relative Density (Specific Gravity) and Absorption of Fine Aggregate, ASTM International, West Conshohocken, PA, 2015, www.astm.org

[85] ASTM C192 / C192M-18, Standard Practice for Making and Curing Concrete Test Specimens in the Laboratory, ASTM International, West Conshohocken, PA, 2018, www.astm.org

[86] ASTM C490 / C490M-17, Standard Practice for Use of Apparatus for the Determination of Length Change of Hardened Cement Paste, Mortar, and Concrete, ASTM International, West Conshohocken, PA, 2017, www.astm.org

[87] ASTM C143 / C143M-15a, Standard Test Method for Slump of Hydraulic-Cement Concrete, ASTM International, West Conshohocken, PA, 2015, www.astm.org

[88] ASTM C138 / C138M-17a, Standard Test Method for Density (Unit Weight), Yield, and Air Content (Gravimetric) of Concrete, ASTM International, West Conshohocken, PA, 2017, www.astm.org

[89] ASTM C39 / C39M-18, Standard Test Method for Compressive Strength of Cylindrical Concrete Specimens, ASTM International, West Conshohocken, PA, 2018, www.astm.org

[90] ASTM C496 / C496M-17, Standard Test Method for Splitting Tensile Strength of Cylindrical Concrete Specimens, ASTM International, West Conshohocken, PA, 2017, www.astm.org

[91] ASTM C78 / C78M-18, Standard Test Method for Flexural Strength of Concrete (Using Simple Beam with Third-Point Loading), ASTM International, West Conshohocken, PA, 2018, www.astm.org

[92] ASTM C1399 / C1399M-10(2015), Standard Test Method for Obtaining Average Residual-Strength of Fiber-Reinforced Concrete, ASTM International, West Conshohocken, PA, 2015, www.astm.org

[93] AASHTO T358-19. Washington, D.C.: American Association of State Highway and Transportation Officials, 2019.

[94] Kahrs, Jason T., David Darwin, and Carl E. Locke. Evaluation of Corrosion Resistance of Type 304 Stainless Steel Clad Reinforcing Bars. Diss. University of Kansas, Civil and Environmental Engineering, 2001.

[95] Trejo, David, Ceki Halmen, and Kenneth Reinschmidt. Corrosion performance tests for reinforcing steel in concrete: technical report. No. FHWA/TX-09/0-4825-1. Texas Transportation Institute, 2009.

[96] ASTM C305-14, Standard Practice for Mechanical Mixing of Hydraulic Cement Pastes and Mortars of Plastic Consistency, ASTM International, West Conshohocken, PA, 2014, www.astm.org

[97] Li, Zongwen, et al. "Properties and Applications of Basalt Fiber and Its Composites." IOP Conference Series: Earth and Environmental Science, vol. 186, Nov. 2018, p. 012052., doi:10.1088/1755-1315/186/2/012052.

APPENDICES

APPENDIX-A : COMPRESSION MACHINE

APPENDIX-B : MACROCELL CORROSION TEST


GPT 16 – 19 Str Cu SAEWe 100Sp
PLANT:
9/25/18
556679
100 FT
Newthein


FLUKE
OFF
COM

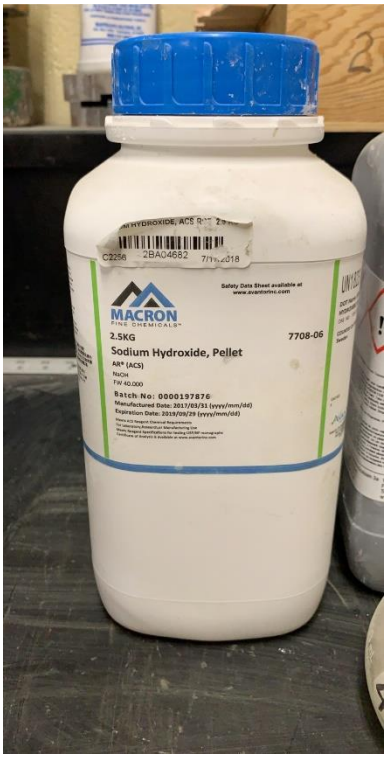
MACRON
FINE CHEMICALS
2.5KG
7708-06
Sodium Hydroxide, Pellet
Batch No: 0000197876

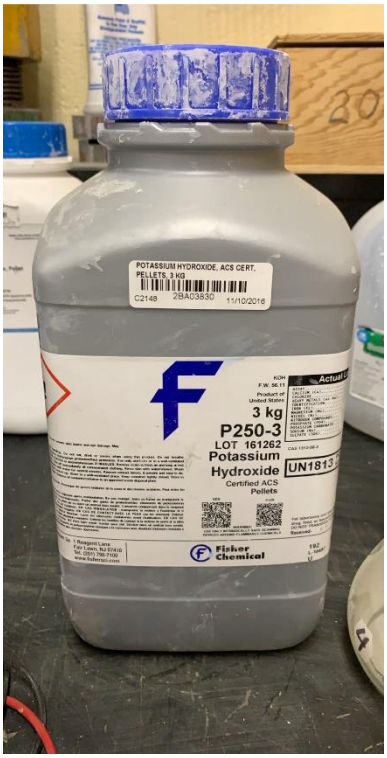
POTASSIUM HYDROXIDE, ACS CERT.
PELLETS, 3 KG
2BA03830
11/10/2016
3 kg
P250-3
LOT 161262
Potassium
Hydroxide
UN1813
Certified ACS
Pellets
Fisher
Chemical

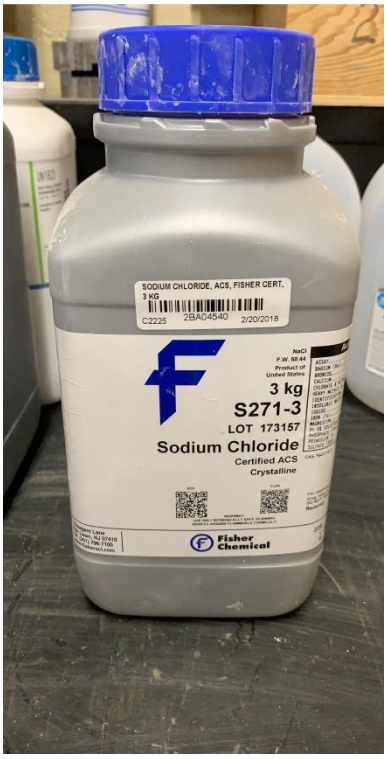
SODIUM CHLORIDE, ACS, FISHER CERT.
3 KG
C2225 2BA04540 2/20/2018
NaCl
F.W. 58.44
Product Of United States
3 kg
S271-3
LOT 173157
Sodium Chloride
Certified ACS
Crystalline
Fisher Chemical

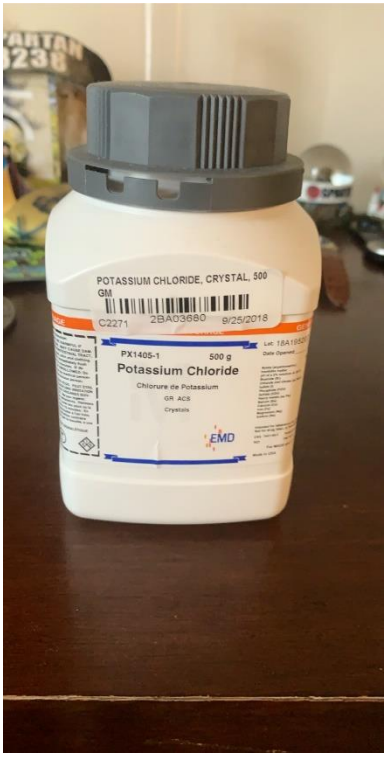
POTASSIUM CHLORIDE, CRYSTAL, 500 GM
C2271 2BA03680 9/25/2018
PX1405-1 500 g
Potassium Chloride
Chlorure de Potassium
GR ACS
Crystals
EMD


SEAWEED SOLUTION LABORATORIES
Agar Agar Powder
15 grams
Preparation:
Step 1: Add 15g Agar Agar for every 1 Liter of Cold, Distilled Water.
Step 2: Stir Periodically & Bring to a Boil.
Step 3: Solution with gel as it cools.
Excellent Gel Strength: 900g/cm²


MA
MA
MA


MB
MB
MB


MA
(15)
MA
(15)
MA
(15)


MB
(15)
MB
(15)
MB
(15)


MA
(30)
MA
(30)
MA
(30)


MB
(30)
MB
(30)
MB
(30)


MA
(45)
MA
(45)


MB
(45)
MB
(45)
MB
(45)


MA
(50)
MA
(50)
MA
(50)


MB
(50)
MB
(50)
MB
(50)